

Isotope effects in chemistry

W. Alexander Van Hook

Abstract. Isotope effects on chemical equilibria, reaction rates and molecular properties are reviewed together with the theoretical formalism for understanding such effects.

Key words: isotope effects • stable isotopes • kinetic isotope effects

Introduction

The term isotope effect (IE) refers to a difference in some molecular or atomic property consequent to a change in mass or mass distribution caused by isotopic substitution. Radioactive and other specific nuclear effects are excluded. Isotopes of a given element are atoms with the same number of protons in the nucleus (atomic number) but different atomic mass (different number of neutrons). Isotope effects, although generally small, are of interest because within the framework of the Born-Oppenheimer approximation the electronic properties of atoms or molecules can be separated from those involving nuclear motion. The electronic structure determines most of the chemistry and much of the physics. It, in turn, is determined by the charges and charge distributions within the atom or molecule of interest and is nearly mass independent. The solution of the electronic part of the problem defines an electronic potential on which nuclear motion occurs. Thus investigation of isotopic substitution amounts to the determination of how mass and/or mass distribution affects motion on the (isotope independent) potential energy surface. Conversely experimental data on IEs can serve as a tool to gain information about the potential energy surface.

For the heavier elements where relative mass differences between isotopes are small, IEs are correspondingly small. For lighter elements relative mass differences are larger as are the IEs. Some representative values are given in Table 1. IEs on equilibrium constants or vapor pressure amount to a few percent or so for H/D substitution (around room temperature (RT)) but are smaller for the heavier elements ($^{12}\text{C}/^{13}\text{C}$

W. A. Van Hook
Department of Chemistry,
University of Tennessee,
Knoxville, TN 37996, USA,
Tel.: 865 588 0951,
E-mail: avanhook@utk.edu

Received: 23 January 2011

Table 1. Some representative isotope effects

System	Process	T (K)	Light/Heavy
$H_2 + 2DI = D_2 + 2HI$	Equilibrium (gas)	600	$K'/K = 1.210$
$^{15}NH_3 + ^{14}NH_4^+ = ^{14}NH_3 + ^{15}NH_4^+$	Equilibrium (solution)	298	$K'/K = 1.034$
$^{10}BF_3(g) + ^{11}BF_3(CH_3)_2O(l) = ^{11}BF_3(g) + ^{10}BF_3(CH_3)_2O(l)$	Equilibrium	298	$K'/K = 1.026$
$^{36}Ar-^{40}Ar$	Vapor pressure	87	$P'/P = 1.006$
H_2O-D_2O	Vapor pressure	373	$P'/P = 1.054$
$C_6H_6-C_6D_6$	Vapor pressure	353	$P'/P = 0.976$
$H_2 + Cl \rightarrow HCl + H^{\cdot}$	Reaction rate	298	$k'/k = 9.6$
$D_2 + Cl \rightarrow DCl + D^{\cdot}$			
$(CH_3)_3CCl \rightarrow (CH_3)_3C^{\cdot} + Cl^{\cdot}$	Reaction rate	298	$k'/k = 2.4$
$(CD_3)_3CCl \rightarrow (CD_3)_3C^{\cdot} + Cl^{\cdot}$			
$^{\cdot}OCH_2CH_2^{35}Cl \rightarrow C_2H_4O + ^{35}Cl^{\cdot}$	Reaction rate	298	$k'/k = 1.008$
$^{\cdot}OCH_2CH_2^{37}Cl \rightarrow C_2H_4O + ^{37}Cl^{\cdot}$			

or $^{235}U/^{238}U$ for example). IEs on rate constants of chemical reaction are typically larger than equilibrium effects (Table 1).

The use of IE studies in the chemical, biological and geological sciences was recently treated by Wolfsberg, Van Hook, Paneth and Rebelo [126]. An important collection of papers treating IEs in chemistry and biology was edited by Kohen and Limbach [65], and Jancso [54] reviewed the field briefly. Melander and Saunders [75], Collins and Bowman [21], Bigeleisen and Wolfsberg [16], and Truhlar [101] have dealt with IEs on chemical reaction rates. Cook [22], Cook and Cleland [23], and Cleland, O'Leary and Northrup [19] discuss IEs on enzyme catalyzed reactions. Hoefs [46] has reviewed stable isotope geochemistry. Criss [25] and Galimov [33] treat the principles of isotope fractionation in nature, while Zarzycki [127] discusses new fields of application for stable isotope studies. Rabinovich [83] describes Russian work on IE's on the physicochemical properties of liquids. Hoepfner [47], Jancso and Van Hook [58], Kiss, Jancso and Jakli [63], and Van Hook [113] have reviewed the field of vapor pressure isotope effects, and Jancso, Rebelo and Van Hook [56] discuss excess properties in solutions of isotopomers and non-ideality in isotopic mixtures [57]. Benedict, Pigford and Levy [9], Cohen [20], Ishida and Fujii [50] and Van Hook [112], among others, have treated the theory and practice of isotope separation. Other reviews on various aspects of isotope science are available. The references above should be regarded as a survey of the available literature. They are not in any way complete, nor do they even contain all of the "important" surveys.

History: from the discovery of isotopes to ~ 1940

It was in the years immediately prior to World War I that the work of Soddy [94] and Fajans [30] on the three natural radioactive decay series (^{238}U to ^{206}Pb , ^{235}U to ^{207}Pb , and ^{232}Th to ^{208}Pb) led independently to the concept of isotopy (Wolfsberg *et al.* [126]). In each series atoms pass from a radioactive progenitor through a long chain of radioactive daughters to a stable lead atom (isotope). Certain of the intermediate daughters differ markedly in their radio-decay properties (different half lives and decay mechanisms) but for all practical purposes are chemically identical, and extremely difficult, if not impossible, to separate one from the other.

Soddy coined the term "isotopes" to distinguish them. The introduction of the concept of atomic number by Van den Broek [107, 108] and Moseley [77] clarified matters, i.e. showed that isotopes differ in atomic mass, not atomic number. After the hiatus caused by World War I, Lindemann and Aston [68] discussed the possibility of separating a mixture of isotopes by distillation, centrifuge, or by producing positive rays and subjecting them to electric and magnetic fields (the method still employed in the mass spectrograph). Also Lindemann [67] reported the first theoretical analysis of the vapor pressure isotope and applied it to earlier efforts to separate isotopes of neon. These efforts led to Aston's development of the mass spectrograph and his use of that instrument to determine the relative masses of the isotopes of neon and chlorine to procure his Nobel Prize (Aston [3]). During the 1920's Aston employed the mass spectrograph to discover no less than 212 of the naturally occurring isotopes. From these results he was able to formulate the whole number rule of atomic structure. Independently, Harkins and Wilson [41-43] working at the University of Chicago made important contributions to the development of the whole number rule. Harkins also worked out the first partial separation of the chlorine isotopes (Harkins and Hayes [40]).

By the late 1920's, although Aston and his colleagues had discovered a large number of isotopic atoms, there was no evidence that the lighter elements hydrogen, carbon, nitrogen and oxygen had isotopes. This was due to the fact that then existing mass spectrographs were too insensitive to detect these isotopes because of their low abundance. A different technique was required. High resolution emission spectroscopic methods in the visible/UV developed by Mulliken [78] were employed by Giaque and Johnston [35, 36], King and Birge [62] and Naude [79] to discover the rare isotopes of oxygen, carbon, and nitrogen respectively. However neither the mass spectrographic nor spectroscopic techniques available at the time permitted characterization of the very low abundance (0.015%) heavy isotope of hydrogen, 2H , known as deuterium, D, even though its existence had been suspected for several years.

Urey, Brickwedde and Murphy [104] set out to discover the heavy isotope of hydrogen. They chose to concentrate their sample by fractional distillation of liquid hydrogen and obtained the atomic spectrum of hydrogen both from tank hydrogen (normal abundance) and the residue from evaporating 4L of liquid hydrogen.

They observed the expected spectral lines for deuterium from both samples but the evaporative residue was much enriched. No evidence of tritium ($^3\text{H} = \text{T}$) was observed. This work led to the award of the 1934 Nobel Prize to Urey. The discovery of deuterium generated a rush of work on deuterium, so much so that Urey and Teal [106] published a sixty page review of the field just a few years later. It is quite understandable that studies of isotope effects were invigorated by the availability of deuterium since the relative mass difference H to D is so much larger than the heavier elements and provides easily measurable isotopic differences. The spurt in IE studies, however, ended around 1940 with the beginning of World War II and the security classification of almost all work in isotope science.

Fundamental theory of isotope effects

The Born-Oppenheimer approximation, molecular vibrations

The interpretation of experimental data on IEs is almost invariably carried out using the Born-Oppenheimer approximation [17] which is employed to determine an isotope independent electronic potential on which nuclear motion occurs. Corrections to this approximation are vanishingly small for atoms heavier than hydrogen, and even there can be ignored except in special circumstances (Bardo and Wolfsberg [4, 5]). The normal starting point considers isolated molecules in the gas phase. Nuclear motion is described in terms of small displacements from the equilibrium positions. The potential energy is approximated with an expansion in terms of displacement coordinates where the leading (quadratic) term is the largest, but cubic and higher terms may contribute. Even so, these higher terms are generally neglected and this leads to a description in terms of a set of $3n-j$ harmonic frequencies (n is the number of atoms in the molecule, $j = 5$ for a linear,

6 for a nonlinear, and 3 for a monatomic molecule). The frequencies can be obtained by diagonalization of the matrix \mathbf{FG} , where \mathbf{F} is an isotope independent ($3n-j$) dimensional potential energy (force constant) matrix and \mathbf{G} is a kinetic energy matrix which takes proper account of mass and mass distribution. Given \mathbf{F} and \mathbf{G} for the set of isotopic molecules one can calculate a complete set of frequencies and isotopic frequency shifts. These can then be employed to evaluate partition functions, partition function ratios, and isotope effects on thermodynamic properties using the methods of statistical thermodynamics. The entire procedure is well suited to machine calculation and Wolfsberg *et al.* [126] give details and appropriate literature references.

In the calculation of thermodynamic properties it is necessary to account for the j zero-frequency rotations and translations which lie at the classical limit in the gas, but take on nonzero values in the condensed phase. One notes that the isotopic frequency shifts are small, at least for isotopes heavier than hydrogen, and it becomes convenient to formulate the isotopic partition function ratios (which lie near unity) by expansion in powers of $1/T$. It has been long established that IE's of the type under discussion vanish in the classical (high temperature) limit and Jacob Bigeleisen and Maria Mayer ([15] 1947, Fig. 1) demonstrated the convenience of defining a reduced partition function ratio, $q_{\text{quantum mechanical}}/q_{\text{classical}}$. This method has the advantage of focusing attention directly on the isotope effects themselves rather than on small differences in the enormously larger values of the partition functions for each species. The Bigeleisen-Mayer approach has long since been widely employed. Waldmann [119] independently proposed an approach similar to the Bigeleisen-Mayer formulation.

The methods outlined above have been applied to a wide variety of special cases including IEs on chemical equilibria, and IEs on rate constants (using transition state theory), vapor pressure, molar volume, etc. Sometimes corrections for anharmonicity, rotation-vibration interaction, centrifugal distortion, and deviations from the Born-Oppenheimer approximation have been



Fig. 1. Jacob Bigeleisen (1919–2010) and Maria Goeppert Mayer (1906–1972). The Bigeleisen-Mayer formalism for the theory of isotope effects has been widely used since its introduction in 1947.

applied. Most analyses consider systems in thermal equilibrium and employ Maxwell-Boltzmann distribution functions. Isotope effects for systems not in thermal equilibrium are also of interest. Non-Maxwellian distributions are important in the treatment of laser methods of isotope separation, IEs on fast unimolecular reactions, etc.

Substituent effects and the first law of isotopics

Studies of the changes in properties when one atom in a molecule is substituted by another (e.g. replacing Cl by Br in CH₃Cl) have been a useful tool of chemists for many years. An isotope effect is a special type of substituent effect. The fact that two isotopomers have the same potential energy surface for nuclear motion to excellent approximation means that isotope effects are theoretically accessible if one knows the potential energy curve. Conversely if one does not know the potential energy curve the isotope effect can be used to learn about the surface. Thus, the Born-Oppenheimer isotope independent potential energy surface is central to the understanding of isotope effects and has been referred to as the First Law of Isotopics.

Isotope exchange equilibria

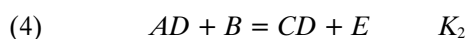
Some examples of IEs on equilibrium constants have been included in Table 1. The Bigeleisen-Mayer [15] treatment introduces the reduced partition function ratio, $(s_2/s_1)f$,

$$(1) \quad \frac{s_2}{s_1} f = \left(\frac{s_2}{s_1} \frac{q_2}{q_1} \right) \prod_i^N \left(\frac{m_{2i}}{m_{1i}} \right)^{-3/2} \\ = \prod_i \frac{u_{2i}}{u_{1i}} \left(\frac{1 - e^{-u_{1i}}}{1 - e^{-u_{2i}}} \right) e^{\frac{1}{2}(u_{1i} - u_{2i})}$$

$$(2) \quad = (\text{PF})(\text{EXC})(\text{ZPE})$$

Subscript 1 refers to the more lightly substituted isotopomer. The definition recognizes that the product of isotopic masses always cancels in the calculation of the IE on the equilibrium constant. It is the same on both sides of the reaction. In Eq. (1) $u_i = hc\nu_i/kT$ and the product is over the $3n-6$ ($3n-5$ if the molecule is linear) normal mode harmonic oscillator frequencies. In these equations s_1 and s_2 are symmetry numbers and cannot lead to any isotope effect. The units of ν_i are cm^{-1} and c is the speed of light. Equation (2) points out the RPFER can be considered as the product of three factors: the product factor (PF), the excitation factor (EXC) and the zero point energy contribution (ZPE). Throughout, the energy zeros are taken at the bottom of the harmonic oscillator wells.

As an example consider the replacement of H by D



so

$$(5) \quad \frac{K_1}{K_2} = \left(\frac{q_{AD}}{q_{AH}} \frac{q_{CD}}{q_{CH}} \right)$$

since A, B, C and E are identical in the two reactions and from the Born-Oppenheimer approximation the two reactions share a common zero. Using Eqs. (1) through (5)



$$(7) \quad \frac{K_1}{K_2} = K_3 = (\text{symmetry number factor})$$

$$\times \frac{\left(\frac{s_2}{s_1} f \right) [AD/AH]}{\left(\frac{s_2}{s_1} f \right) [CD/CH]}$$

where the symmetry number factor is $((s_{AH}/s_{AD})/(s_{CH}/s_{CD}))$. The IE is the product of the symmetry number factor and terms which depend only on normal mode vibrational frequencies. The introduction of the RPFER had a profound effect on IE studies. Equation (1) focuses attention of the isotope dependent frequencies and the isotope independent force constants which define those frequencies. Isotope effects reflect force constant differences at or near the position of isotope substitution on the two sides of the reaction.

Limiting values: the low and high temperature limits

At low temperature u_i increases, $(1 - e^{-u_i}) \rightarrow 1$ and RPFER $= (s_2/s_1)f = (\text{PF})(\text{EXC})(\text{ZPE}) \rightarrow \prod (u_{2i}/u_{1i}) (\exp[-(u_{2i} - u_{1i})/2])$. No upper vibrational levels are populated; this condition is known as the zero point energy approximation, or, alternatively, as the low temperature approximation. For a typical CH stretching frequency, $\nu \sim 3000 \text{ cm}^{-1}$, $u \sim 4$ at 1050 K and it is reasonable to use the ZPE approximation for that frequency at temperatures below 1000 K. To the same precision for $\nu \sim 300 \text{ cm}^{-1}$, $u \sim 4$ around 100 K and the ZPE approximation is only useful below that temperature. Note that at very low temperature IEs can get very large.

At high temperature $u_i = hc\nu_i/kT$ and in Eq. (1) $\text{ZPE} = e^{u_i/2} \rightarrow e^0 = 1$. Also $1 - e^{-u_i} \sim 1 - (1 - u_i + u_i^2/2 + \dots) \sim u_i$, so

$$(8) \quad \lim_{u \rightarrow 0} \prod_i \frac{u_{2i}}{u_{1i}} \left(\frac{1 - e^{-u_{1i}}}{1 - e^{-u_{2i}}} \right) = \prod_i \frac{u_{2i}}{u_{1i}} \frac{u_{1i}}{u_{2i}} = 1$$

and, overall, $(s_2/s_1)f$ approaches unity. Thus at high temperature the limiting equilibrium constant IE, Eq. (7), is given by a ratio of symmetry numbers. The symmetry number ratio is a purely statistical factor and will not lead to any enrichment of isotopes. There are no isotope effects in the classical high temperature limit.

One can explore the approach to the high temperature limit by carrying additional terms in the expansions of $e^{u_i/2}$ and $1 - e^{-u_i}$, in this fashion obtaining

Table 2. Spectroscopic properties needed to calculate K_{eq} for $\text{H}_2 + 2\text{DI} = \text{D}_2 + 2\text{HI}$

Molecule	ω_e/cm^{-1} ^(a)	$\omega_e x_e/\text{cm}^{-1}$ ^(b)	B_0/cm^{-1} ^(b)	σT ^(b)
H ₂	4405.3	125.3	59.3	85.4
D ₂	3117.1	63.0	29.9	43.0
HI	2309.5	39.7	6.5	9.3
DI	1640.2	20.0	3.3	4.7

^(a) Harmonic frequency.

^(b) Parameters required for anharmonic corrections. E.g. Wolfsberg [125].

$$\begin{aligned}
 (9) \quad \frac{s_2}{s_1} f &= \prod_i^{3N-6} \frac{\varphi(u_{1i})}{\varphi(u_{2i})} = \prod_i^{3N-6} \frac{\left(1 + \frac{u_{1i}^2}{24}\right)}{\left(1 + \frac{u_{2i}^2}{24}\right)} \\
 &= 1 + \sum_i \frac{1}{24} (u_{1i}^2 - u_{2i}^2) \\
 &= 1 + \frac{1}{24} \left(\frac{h}{kT}\right)^2 \sum_i (v_{1i}^2 - v_{2i}^2)
 \end{aligned}$$

Thus, the first order correction to classical (high temperature) statistical mechanics is proportional to h^2 (Wigner [122]).

An example, $\text{H}_2 + 2\text{DI} = \text{D}_2 + 2\text{HI}$

The vibrational frequencies needed to calculate this exchange equilibrium constant are given in Table 2. To good enough approximation $u_2 = u_1/2^{1/2}$ for both the H₂/D₂ and the HI/DI pairs.

$$(10) \quad K = [(s/s') f(\text{H}_2/\text{D}_2)] / [(s/s') f(\text{HI}/\text{DI})]^2$$

In each case the prime refers to the lighter isotope. At all but very high temperatures it is necessary to employ the complete equation because the vibrational frequencies for all four molecules are quite high. At room temperature $u(\text{H}_2) \sim 21$ and $u(\text{HI}) \sim 11$. The results of the calculation are shown in Fig. 2. At very high temperature Eq. (9) may be used and the exchange constant is

$$(11) \quad K = 1 + (1/24)(1 - 1/2^{1/2})(v^2(\text{H}_2) - v^2(\text{HI}))(hc/k)^2/T^2 + \dots = 1 + 3.55 \times 10^5/T^2 + \dots$$

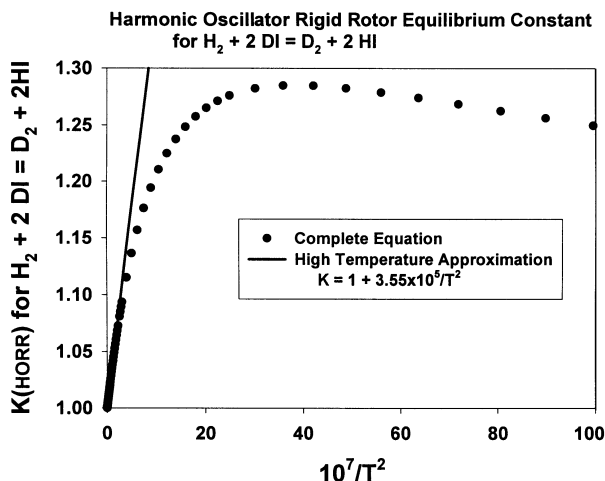


Fig. 2. Harmonic oscillator rigid rotor equilibrium constant for $\text{H}_2 + 2\text{DI} = \text{D}_2 + 2\text{HI}$.

This result is shown in Fig. 2. More precise calculations include corrections for nonclassical rotation and vibrational anharmonicity. The corrections lower the calculated isotope effects by only several percent. The calculated IEs are in good agreement with experiment.

Corrections to the Bigeleisen-Mayer equation. The nuclear field shift effect

Several corrections to the Bigeleisen-Mayer equation need to be considered. The most important is the correction for anharmonicity (Wolfsberg [125]). Anharmonic zero point corrections are only important for vibrations involving light atoms. They account for changes of at most 1% or so in logarithmic fractionation factors calculated for exchange between molecular species containing H, D or T. Two other corrections arise from the use of the Born-Oppenheimer approximation. The first, the adiabatic correction (Bardo and Wolfsberg [4, 5]), arises from the coupling between electronic and nuclear motion and, again, is only important for reactions involving hydrogen isotopomers. It is completely negligible for heavier atoms because it scales proportionally to $\delta M/M^2$. The second arises from a shift in electron energy states in an atom or molecule due to the perturbation of those electrons with high charge density at the nucleus. This, the field shift correction, depends on nuclear size and shape. Since the electron is bound more strongly to the smaller (lighter) nucleus with its higher charge density, the ground state of the heavier isotopomer will lie higher than the one for the lighter isotopomer. **This is opposite to the ordering of the zero point energies associated with molecular vibrations**, but until the late 1980's it was not suspected that the effects were large enough to affect thermodynamic isotope effects. Fuji and coworkers [31], however, reported anomalies in separation factors for the (uranium-IV/uranium-VI) red-ox exchange reaction between ^{238}U and lighter uranium isotopes. Interestingly the separation factors for odd/even ($^{233}\text{U}/^{238}\text{U}$ and $^{235}\text{U}/^{238}\text{U}$) pairs lie significantly above the correlation lines for the even/even ($^{234}\text{U}/^{238}\text{U}$ and $^{236}\text{U}/^{238}\text{U}$) pairs. According to the Bigeleisen-Mayer formalism all the separation factors should scale proportionally to the mass difference ($^{238}\text{U}-^i\text{U}$). The anomaly lies well outside the experimental error. It was Bigeleisen [12] who demonstrated the ($^i\text{U}/^{238}\text{U}$) separation factors can be written as the sum of vibrational (Bigeleisen-Mayer) and field shift contributions. He theoretically calculated the isotope independent scaling factor which defines the mass dependence of the field shift term thus explaining the anomaly. **It is interesting and important to recognize that the field shift and Bigeleisen-Mayer**

contributions are of opposite sign. For the uranium system the field shift makes the largest contribution to the separation factor. The vibrational contribution leads to a preference for the heavier isotope in the U(VI) species, while the larger field shift effect prefers the heavy isotope in the U(IV) species. The net effect is a preference of the heavy isotope in U(IV). The anomalous odd/even behavior is due to the fact that the ^{233}U and ^{235}U isotopomers have nuclear quadrupole moments, the even mass isotopomers do not. Consequently the field shift does not scale proportionally to mass difference. Field shift contributions to redox separation factors have been observed for other metal systems. They only need to be considered for cases involving atoms with high nuclear charge densities (heavy metals).

Kinetic isotope effects

Transition state theory of isotope effects

The basic idea employed in the transition state theory of chemical reactions as developed by Eyring and others is diagrammed in Fig. 3 (Glasstone, Laidler and Eyring [37]), Bigeleisen and Wolfsberg [16], Van Hook [110], Wolfsberg *et al.* [126]). The reaction takes place on a $3n$ dimensional isotope independent electronic potential energy surface (n the total number of atoms in the system). One of these dimensions, the reaction coordinate, corresponds to the minimum energy path between the minima characterizing reactant and product. The transition state lies in a saddle point at the maximum, ΔE^\ddagger , of this minimum energy path. Energies are measured from the potential energy minima. The reaction can proceed semi-classically along the reaction coordinate, over the barrier and its transition state, to product, or, alternatively by quantum mechanical tunneling through the barrier with (generally) smaller

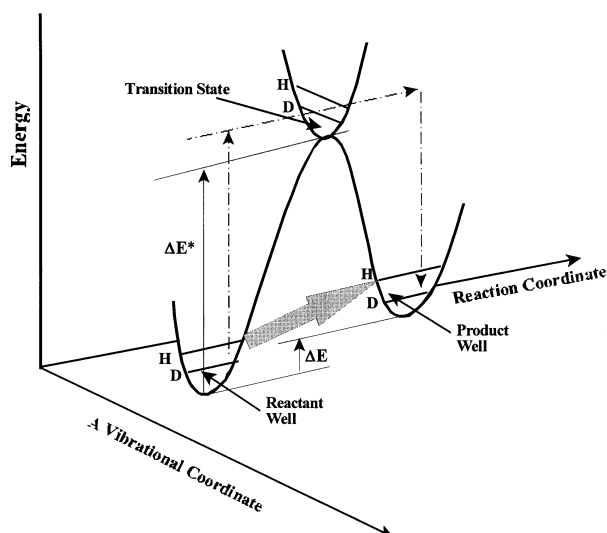


Fig. 3. Energetics of a reaction (schematic). The Born-Oppenheimer energy surface is mapped onto the reaction coordinate. One of the $3n-6$ vibrational modes orthogonal to the reaction coordinate is shown for the transition state. H and D zero point levels are indicated. The semiclassical reaction follows the dash-dot arrows, but some fraction may proceed by tunneling (gray arrow).

probability. Note that the curvature along the reactant coordinate is negative. Motion along this coordinate will be treated separately.

We now consider a chemical reaction



The rate constant, k , is defined by the relation $-d[A]/dt = k[A][B]$ and is not to be confused with the Boltzmann constant, k (or k_B where the use of “ k ” would lead to confusion). The square brackets denote concentrations. A central assumption of transition state theory is that equilibrium is maintained between reactants and transition state. Thus the rate of reaction is given by the equilibrium concentration of transition state $[AB^\ddagger]$ multiplied by the rate of decomposition of the transition state, r , and by κ the probability of motion in the forward direction (to products) rather than reverse (to reactants).

$$(13) \quad -\frac{d[A]}{dt} = rK^\ddagger\kappa[A][B]$$

where $K^\ddagger = [AB^\ddagger]/([A][B])$ is the equilibrium constant between reactants and transition state. The factor r is evaluated using the one dimensional translational partition function which treats motion along the reaction coordinate. One obtains

$$(14) \quad k = \frac{k_B T}{h} K^\ddagger \kappa$$

where K^\ddagger has been replaced with K'^\ddagger to indicate these later expressions for the partition function now contain only $3n^\ddagger-7$ ($3n^\ddagger-6$ if linear) real vibrations. Of course the reactant partition functions are treated using $3n-6$ real vibrations for each A and B species. The parameter κ (which may be significantly large) is dominated by tunneling. A brief discussion of tunnel effects is deferred to a later section. The isotope effect on the rate constant is

$$(15) \quad \frac{k_1}{k_2} = \frac{K_1'^\ddagger \kappa_1}{K_2'^\ddagger \kappa_2}$$

with 1 and 2 referring as usual to isotope substitution, say A_1 and A_2 and their corresponding transition states, A_1B^\ddagger and A_2B^\ddagger . Introducing partition functions for reactants and transition states

$$(16) \quad \frac{K_1'^\ddagger}{K_2'^\ddagger} = \frac{(q_{A_2} q_B / q_{A_1} q_B)}{(q'_{A_2 B^\ddagger} / q'_{A_1 B^\ddagger})} = \frac{(q_{A_2} / q_{A_1})}{(q'_{A_2 B^\ddagger} / q'_{A_1 B^\ddagger})}$$

The reduced partition function ratio for the transition state is then straightforwardly

$$(17) \quad \left(\frac{s_2}{s_1}\right) f^\ddagger = f^\ddagger = \prod_i^{(3N^\ddagger-6)} \frac{u_{2i}^\ddagger}{u_{1i}^\ddagger} \left(\frac{1-e^{-u_{1i}^\ddagger}}{1-e^{-u_{2i}^\ddagger}}\right) e^{(u_{1i}^\ddagger - u_{2i}^\ddagger)/2}$$

Because the reaction coordinate has been treated separately the product is over $3n^\ddagger-7$ rather than $3n^\ddagger-6$ coordinates. For nonlinear transition states there are $3n^\ddagger-6$ coordinates. The ratio of isotopic rate constants is

$$(18) \quad \frac{k_1}{k_2} = (\text{symmetry number factor}) \\ \times \frac{v_{1L}^\ddagger \left(\frac{s_2}{s_1} f\right) (A_2/A_1)^{\kappa_1}}{v_{2L}^\ddagger \left(\frac{s_2}{s_1} f^\ddagger\right) (A_2 B^\ddagger / A_1 B^\ddagger)^{\kappa_2}}$$

As before, symmetry number factors do not lead to isotope enrichment.

The use of the RPFRR to study kinetic isotope effects was first undertaken by Bigeleisen [10], this work was elaborated by Bigeleisen and Wolfsberg [16]. It has since been applied to a plethora of reactions.

Modern methods to calculate RPFRRs, isotope equilibrium constants, and kinetic isotope effects

Spectroscopic data are available for a large number of molecules, including isotopically labeled molecules, and it would appear straightforward to employ such data to calculate $(s_1/s_2)f$ for reactants and products in chemical equilibria and rate expressions. This has proved to be unsatisfactory. Except for the simplest molecules some normal mode frequencies are spectroscopically forbidden or not observed for other reasons. Also the precision of vibrational frequency measurements is often insufficient to permit calculation of RPFRR at useful precision. Moreover observed frequencies are anharmonic and the corrections needed to produce sets of harmonic frequencies are troublesome. For these reasons it is customary to employ the experimental frequencies to deduce a set of isotope independent force constants which, on the one hand, are consistent with the spectroscopic data, and on the other can be employed to calculate a self consistent set of harmonic frequencies for all isotopomers, and thence high precision isotope frequency shifts and RPFRRs. Typically some variant of the Wilson, Decius, Cross [123] **FG** method is employed for this purpose. This approach is well suited for modern computational methods and computer programs for that purpose were introduced by Schachtsneider and Snyder [88], then adapted to IE studies by Stern and Wolfsberg [96] who made a thorough study of the relationship between force constant changes (reactant to product, or reactant to transition state) and the calculated isotope effects. More recently computations have moved back a step further toward fundamental theory. They begin with an *ab initio* quantum mechanical calculation of the Born-Oppenheimer surface (Wolfsberg *et al.* [126]), Cramer [24]. The Born-Oppenheimer surface is probed in the vicinity of the minima and saddle points to establish gradients and force constants for the reactant(s) and transition state. This involves the calculation of the energy at numerous points along each coordinate and is computationally intensive. One commonly used program is Gaussian03 but a number of other programs are available. The details are highly technical and will not be explored in this review. Many examples of theoretically calculated isotope effects described in this or other reviews or cited in the tables have employed these general procedures.

Variational transition state theory

In spite of the many successes of transition state theory (TST) it is inadequate for a proper treatment of reaction kinetics. Ordinary TST is not capable of correctly describing quantum effects and barrier penetration (tunneling). A more general theory, variational transition state theory (VTST), developed by Truhlar and coworkers [101], Allison and Truhlar [2] optimizes the location of the surface dividing reactants from products, placing it so that forward flux is minimized. The basic idea is to find a dividing surface which leads to a higher free energy of activation and thus a lower rate constant. In TST the dividing surface is defined geometrically as the saddle point on the Born-Oppenheimer surface, but in VTST it is that surface which leads to the minimum value of the rate constant. In considerations of isotope effects the potential surface is isotope independent in both TST and VTST. In TST the transition state for both isotopes is at the saddle point, but for VTST the transition point need not be (and usually is not) at the saddle point, and may be different for the two isotopes. As a consequence the expression for the isotope effect on a rate constant k_1/k_2 must include a factor involving the energy differences of the isotopic dividing surfaces. Additionally, the force constants from which the vibrational frequencies of the isotopic transition states are calculated, and the geometries of the transition states, may differ a bit. These points reemphasize the fact that TST is much simpler conceptually than VTST. There is just one transition state in TST and it is located at the saddle point on the minimum energy path. In VTST the dividing surface for each isotopomer is temperature dependent (since the partition functions and consequently the free energy of activation are temperature dependent).

Tunneling

It is well understood that a chemical reaction can occur even for a system whose energy is less than the barrier height. This purely quantum mechanical phenomenon is referred to as tunneling. The probability of tunneling decreases as the energy deficit for classical passage increases and as the length of the tunneling path increases. Also light particles have much higher tunneling probability than do heavier ones. As it turns out then, tunneling is most important for the transfer of light particles (H, H⁺ or H⁻ vs. D, D⁺ or D⁻) through narrow barriers. Kohen [64] has described the observational criteria generally used to determine whether or not tunneling is an important factor in determining isotope effects on any particular reaction or reaction sequence.

In both TST and VTST tunneling is introduced as a correction factor, generally denoted κ . In TST tunnel corrections are sometimes calculated using the Wigner $u^2/24$ law [122], see Eq. (9).

$$(19) \quad \kappa = 1 - u^{\ddagger 2}/24 + \dots$$

In this equation u^{\ddagger} is the reduced (imaginary) frequency which describes barrier curvature. Much better and much more widely used approximations were introduced

by Bell (parabolic barrier) and by Eckart. The Bell and Eckart expressions each lead to exactly soluble quantum mechanical expressions for the barrier reflection and transmission probabilities. Details are available elsewhere (Wolfsberg *et al.* [126]), Melander and Saunders [75].

In the complete VTST calculations the tunneling factor is set equal to the ratio of the temperature averaged quantum transmission coefficient and the corresponding classical transmission coefficient. The quantum mechanical tunneling problem can be solved exactly for the three atom collinear case (and even for

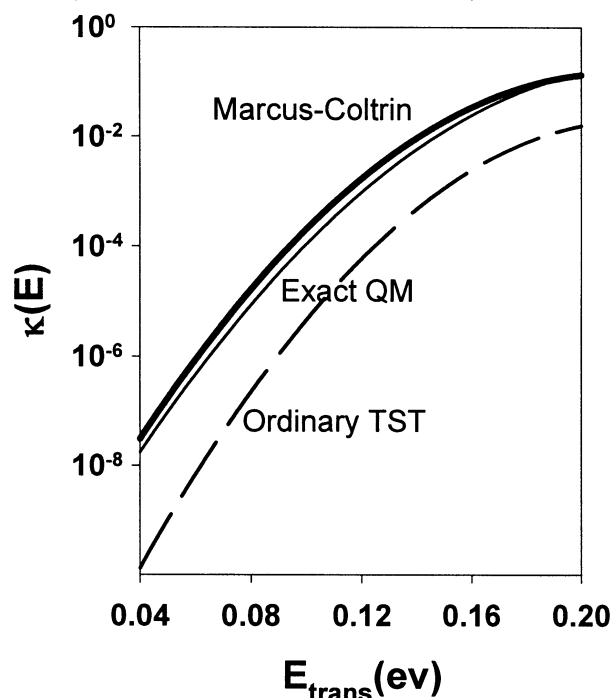


Fig. 4. Reaction probability vs. initial translational energy for the $H + HH = HH + H$ surface. Exact quantum mechanical calculations are compared with the Marcus-Coltrin multidimensional tunneling approximation and with ordinary TST (Marcus and Coltrin [73]).

Table 3. Tests of TST and VTST by comparing with exact quantum calculations; isotope effects at 300 K. The numbers in the table are ratios of rate constants for the two selected reactions (Allison and Truhlar [2])

Reaction	k_H/k_D		
	TST	Best VTST	Exact
$H + HH \rightarrow HH + H$	1.33	3.85	4.35
$D + HH \rightarrow DH + H$			
$H + DD \rightarrow HD + D$	0.62	0.60	0.57
$D + DD \rightarrow DD + D$			
$H + FF \rightarrow HF + F$	1.33	1.56	1.61
$D + FF \rightarrow DF + F$			
$Cl + HCl \rightarrow ClH + Cl$	7.25	6.27	5.37
$Cl + DCl \rightarrow ClD + Cl$			

Table 4. Temperature dependence of the hydrogen isotope reaction, $D + HH \rightarrow DH + H$ and $H + DD \rightarrow HD + D$

T (K)	$k_{D,HH}/k_{H,DD}$	
	Calculated ^a	Experiment ^b
200	74	—
300	16	15
400	7.9	7.6
800	2.7	2.8

^a Mielke *et al.* [76].

^b Ridley *et al.* [86].

the corresponding three dimensional case) but the general problem is still very difficult mathematically. Marcus and Coltrin [73] and Truhlar [101] describe calculations of multidimensional tunneling factors which yield reaction probabilities in excellent agreement with the exact quantum mechanical values. An example is given in Fig. 4.

Tests of VTST (including tunneling)

Table 3 shows comparisons of TST and VTST calculations of IEs for collinear reactions with the exact quantum mechanical calculations. Table 4 compares experimental and VTST calculated values for $D + H_2 = (D-H-H)^\ddagger = DH + H$ and $H + D_2 = (H-D-D)^\ddagger = HD + D$. The excellent agreement between theory and experiment is gratifying. Table 5 compares experimental and calculated IEs for some enzyme reactions. Tables 3, 4 and 5 clearly demonstrate that the VTST theory is superior to TST especially for light atom transfer. Nonetheless the fact remains that TST is adequate to rationalize the basic features of the isotope effects. For that reason it remains in widespread use for interpretation of experimentally measured isotope effects. This is because the computational complexity of VTST often outweighs its practical implementation. VTST calculations are far more tedious and expensive, and VTST packages for computer implementation are not so widely available as those for TST.

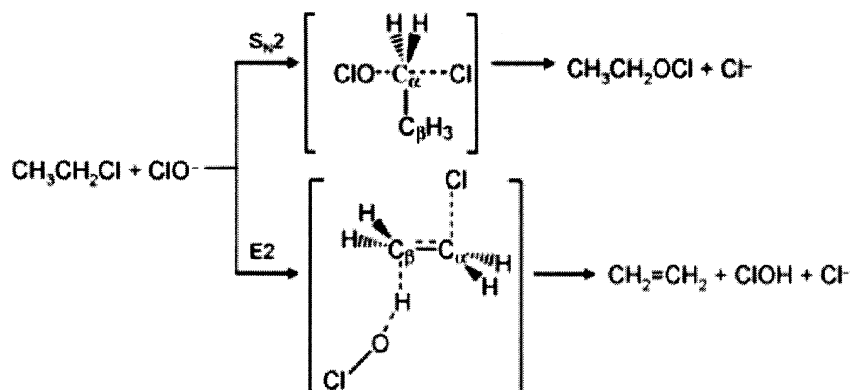
Kinetic isotope effects continued

Primary and secondary IEs

Primary kinetic isotope effects are those in which the bond to the isotopically substituted atom is broken (or otherwise directly changed) in the course of the reaction.

Table 5. Experimental and calculated isotope effects for several enzyme systems^a

Enzyme	KIE	TST	Best VTST	Experiment
Enolase	Primary H/D	4.7	3.5	3.3
LADH	Primary H/T Secondary H/T	6.6 1.08	6.9 1.27	7 to 8 1.36
MADH	Primary H/D	5.9	18	17

^aTruhlar [101].**Fig. 5.** Reaction pathways for hypochlorite plus ethyl chloride (Villano *et al.* [117]).

Secondary kinetic isotope effects are those in which the isotope substitution occurs at position(s) away from the bonds being made or broken. For example in the second order S_N2 reaction of hypochlorite and ethyl chloride



the isotopic ratio $[k(^{35}\text{Cl})/k(^{37}\text{Cl})]$ corresponds to a primary chlorine isotope effect, while $[k(\alpha\text{-H}_2)/k(\alpha\text{-D}_2)]$ corresponds to an α (alpha) deuterium secondary isotope effect ($\alpha = 1$ bond between the position of isotope substitution and the reacting bond, $\beta = 2$ bond separation, etc.). Secondary IEs have been reviewed by Hengge [44]. Typically they are markedly smaller than primary effects and are often inverse. They fall off in the order $\alpha > \beta > \gamma$, etc. Secondary IEs for S_N1 solvolysis reactions generally lie in the range 10 to 25% per D. The rationalization originally proposed by Streitweiser *et al.* [97] is generally accepted. In this explanation the change from sp^2 to sp^3 at the α -carbon on formation of the carbonium ion transition state is accompanied by changes in force constants and vibrational frequencies involving the carbon, particularly the out-of-plane bending mode which is significantly red shifted in the transition state. These ideas have been confirmed by machine calculations (Stern and Wolfsberg [96]), Shiner *et al.* [92]. The existence of β and/or γ 2° IEs has been sometimes rationalized using arguments based on hyperconjugative or steric effects. As a cautionary note it is important to point out such arguments are completely equivalent to the standard interpretation of KIEs in terms of isotope independent force constants, reactant to transition state.

Relative isotope effects: the Swain-Schaad relation

It is often useful to make comparisons of KIEs for multiple pairs of isotopes of the same element, say H/D vs. H/T. The relationship between $k_{\text{H}}/k_{\text{D}}$ and $k_{\text{H}}/k_{\text{T}}$ is

approximately described by the Swain-Schaad equation (Swain *et al.* [98])

$$(21) \quad (k_{\text{H}}/k_{\text{T}}) = (k_{\text{H}}/k_{\text{D}})^{1.44}$$

In deriving Eq. (21) one assumes the H, D and T motions can all be treated in the ZPE approximation and the only important isotope sensitive motions are the stretching modes. These drastic assumptions imply the result is can only be used for qualitative purposes. Hirschi and Singleton [45] have discussed deviations from the Swain-Schaad relation for reactions without tunneling or kinetic complexity.

Isotope effects as probes for reaction path and/or transition state structure

It has long been argued that IE studies provide insight into the structure of the transition state, a property not amenable to direct experimental observation. Two examples chosen from the multitude available in the literature follow.

Figure 5 illustrates competitive reaction paths for the reaction of hypochlorite anion with ethyl chloride. At the top hypochlorite attacks ethyl chloride by a second order nucleophilic displacement (S_N2) process, while at the bottom hypochlorite abstracts a proton as chloride is eliminated (E2). This reaction has been thoroughly studied in both the gas and condensed phases. Gas phase data for a series of alkyl chlorides are shown in Table 6.

Table 6. Deuterium KIEs for the gas phase reaction between RCl and ClO^- at room temperature (Villano *et al.* [117])

RCl	KIE
$\text{CH}_3\text{Cl}/\text{CD}_3\text{Cl}$	0.85
$\text{C}_2\text{H}_5\text{Cl}/\text{C}_2\text{D}_5\text{Cl}$	0.99
$i\text{-C}_3\text{H}_7\text{Cl}/i\text{-C}_3\text{D}_7\text{Cl}$	1.70
$t\text{-C}_4\text{H}_9\text{Cl}/t\text{-C}_4\text{D}_9\text{Cl}$	2.31

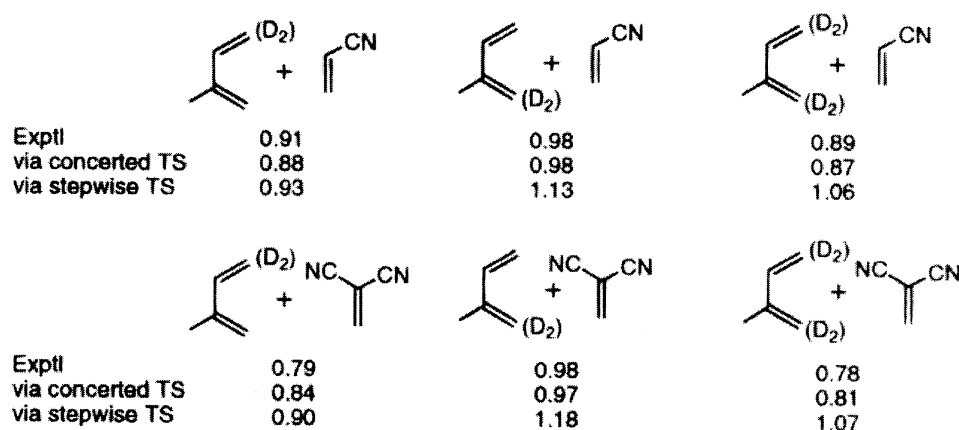


Fig. 6. Experimental (top rows) (Gajewski *et al.* [32]) and calculated (Houk *et al.* [48]) secondary deuterium isotope effects, k_H/k_D (per D) for concerted and stepwise Diels-Alder reactions.

Complications due to solvent interaction with the reactant and transition states are thus avoided, but it is interesting to note that the IEs in Table 6 are about the same as those in aqueous solvent. The reaction of ClO^- with methyl chloride can only proceed via $\text{S}_{\text{N}}2$, while that with *t*-butyl chloride proceeds via E2 (since $\text{S}_{\text{N}}2$ attack on the Cl substituted carbon is blocked). The isotope effects for the intermediate compounds thus measure the relative contributions of the two paths; E2 becomes the dominant channel with increasing steric hindrance.

Figure 6 compares experimental and calculated 2° deuterium IEs for the Diels-Alder pericyclic addition reaction between 2-methyl butadiene and cyanoethylene (top) and 1,1-dicyanoethylene (bottom). TST calculations were carried out for potential energy surfaces corresponding to stepwise and concerted transition states. The agreement between experiment and calculation for the concerted case is excellent and clearly establishes the mechanism as concerted.

Solvent isotope effects

It is reasonable to expect that isotope substitution on solvent molecules will affect both equilibrium and rate constants. Most solvent IE studies have been carried out in aqueous media because deuterated (heavy) water is generally available at an affordable price, but also because almost all reactions of biochemical interest occur in water solution.

The isotope effect on the acid dissociation constants of H_2O and D_2O has been carefully measured by Paabo and Bates [81]), $2\text{H}_2\text{O} = \text{H}_3\text{O}^+ + \text{OH}^-$ and $2\text{D}_2\text{O} = \text{D}_3\text{O}^+ + \text{OD}^-$

$$(22) \quad \Delta pK_a = -\log[(\text{D}_3\text{O}^+)(\text{OD}^-)] - (-\log[(\text{H}_3\text{O}^+)(\text{OH}^-)]) = 0.958$$

Thus the acid dissociation constant of ordinary water is about ten times larger than that of heavy water. This is a significant isotope effect and has important consequences. On the other hand the acid dissociation constant of numerous weak organic acids scatter widely, $\langle \Delta pK_a \rangle = 0.5 \pm 0.1$; on average organic acids dissolved in D_2O are only about 30% as dissociated as their sister compounds dissolved in H_2O .

Many rate constants in aqueous solutions are pH or pD sensitive. Enzyme catalyzed reactions often show maxima in plots of pH (or pD) vs. rate (bell shaped curves). Consequently it is important to compare isotopic rate effects at equivalent positions on the curves (equivalent acidities). Also both equilibrium and rate constants are expected to vary in a nonlinear fashion with solvent atom fraction D (Fig. 7). For solvent KIEs one can use such nonlinearities to deduce information about the number of protons actively participating in the transition state (Quinn [82]).

Isotope effects on enzyme catalyzed reactions

One of the most active areas of isotope science in recent years has been the application of KIE theory and experiment to the elucidation of reaction paths and transition state and active site structures of enzyme catalyzed reactions (Cook [22], Cook and Cleland [23], Cleland, O'Leary and Northrup [19], Truhlar [101]). Space does not permit a review of this important field of research. Very briefly, however, we mention, for example, that Cleland [18] has reviewed (the elucidation) of enzyme mechanisms from isotope effects, while Warschel *et al.* [120] discuss computer simulations of IEs in enzyme

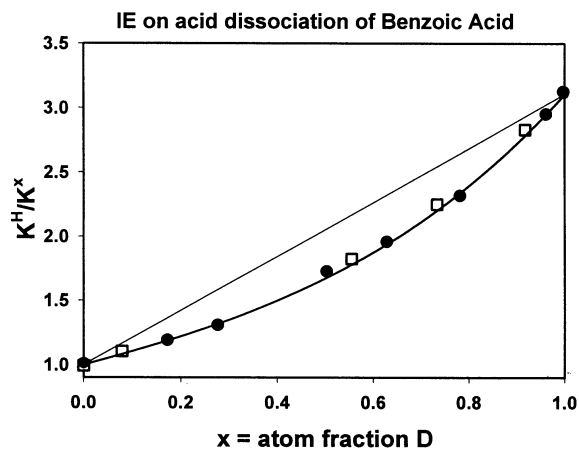


Fig. 7. The IE on acid dissociation constants of benzoic acid $\text{C}_6\text{H}_5\text{COOL}$ ($\text{L} = \text{H}$ or D) vs. atom fraction D of the solvent (Lowe and Smith [70]). The points are experimental. The bottom line is theoretically calculated, the upper line shows the linear approximation.

catalysis, Roth and Klinman [87] treat oxygen-18 isotope effects as a probe of enzyme activation of molecular oxygen, Kohen [64] deals with KIEs as probes for hydrogen tunneling in enzyme catalysis, and Northrop [80] discusses the effect of hydrostatic pressure on IEs of enzyme reactions. As throughout this review the citations are illustrative, not exhaustive.

Condensed phase isotope effects

In this section we discuss IEs on physical properties such as vapor pressure, molar volume, compressibility, heats of vaporization, freezing points, and so forth, for liquids, solids and solutions. Some properties like the vapor pressure isotope effect, VPIE, for example, are of great practical interest because they form the basis for isotope separation processes. Of equal interest is the fact that condensed matter isotope effects are closely related to the intermolecular forces which cause condensation and therefore serve as useful probes to test ideas about the nature of condensation and the motions of molecules in condensed phases. Earlier reviews include those of Wolfsberg *et al.* [126], Van Hook [113], Jancso and Van Hook [58], Rabinovich [83], Jancso, Rebelo and Van Hook [56, 57], and Bigeleisen, Lee and Mandel [14] among others.

The vapor pressure isotope effect, VPIE

The vapor pressure of liquids and solutions is related to the free energy of the condensed phase in a simple fashion. The VPIE is obtained by equating partial molar free energies in condensed and vapor phases remembering $[\mu_i^l(c) - \mu_i(c)] = [\mu_i^l(v) - \mu_i(v)]$. This leads straightforwardly (Bigeleisen [11]) to

$$(23) \quad \ln(P'/P) = \text{VPIE} = \ln(f_c'/f_g) - (B'P' - BP) + (P'V' - PV)_c / RT = \ln(Q_v'Q_c/Q_vQ_c') - (B'P' - BP) + (P'V' - PV)_c / RT$$

The equation applies to comparisons between separated isotopes. The prime refers to the lighter isotope and the Q s are properly averaged partition functions for the vapor and condensed phases. The last two terms on the right hand side are corrections for nonideality in the vapor phase, (B' and B are vapor phase second virial coefficients in the pressure expansion, $PV/(RT) = 1 + BP + \dots$), and for isotopic differences in the condensed phase molar volumes, respectively. At low enough temperatures, say at or below the normal boiling point, $\sim 0.7T_{\text{critical}}$, the last two terms are small and to good approximation the VPIE defines the condensed phase reduced partition function ratio, $\text{VPIE} = \ln(f_c'/f_g)$.

When considering the liquid-vapor equilibrium of a mixture of isotopes one normally defines fractionation factors α and α''

$$(24) \quad \alpha = (y/y')/(x/x') \quad \text{and} \quad \alpha'' = 1/\alpha = (y'/y)/(x'/x)$$

Here x and y denote mole fractions in the liquid and vapor respectively. To excellent approximation we obtain

$$(25) \quad \ln \alpha'' = \ln(f_c'/f_g) + \ln(\gamma'/\gamma) = \ln(Q_v'Q_c/Q_vQ_c') + \ln(\gamma'/\gamma)$$

In the last term γ' and γ are activity coefficients in the condensed phase. Fractionation experiments are often carried out with the rare isotope at high dilution. In that case the other isotope, say for example the unprimed one, is ideal in the Raoult's law sense, $\gamma = 1$, and the result is particularly simple

$$(26) \quad \ln \alpha'' = \ln(f_c'/f_g) + \ln(\gamma') = \ln(Q_v'Q_c/Q_vQ_c') + \ln(\gamma')$$

Note that $RT \ln \gamma'$ is the free energy of transfer of the primed isotope from its pure liquid (i.e. its Raoult's law standard state) to infinite dilution in the unprimed solvent (the Henry's law standard state). Very often this last term is small enough to be ignored.

In order to implement Eqs. (25) and (26) Stern, Van Hook and Wolfsberg [95] successfully applied the harmonic oscillator rigid rotor model to both condensed and vapor phases for the deuterated ethylenes. That approach has since been widely used. Van Hook [109] extended the method, improving agreement with the temperature dependence of the VPIE by treating the condensed phase external frequencies using pseudo-harmonic Gruneisen lattice theory.

The AB approximation

It is useful to have an approximate relation for VPIE, especially when complete vibrational analysis is impossible. The AB approximation serves that purpose and sometimes gives more physical insight than do detailed but very complicated calculations using Eqs. (25) and (26).

$$(27) \quad \ln(f_c'/f_g) = A/T^2 + B/T$$

The approximation is based on the fact that ordinarily condensed phase vibrations fall into a high frequency B group, most often the internal modes where $u_i = hc\nu_i/kT \gg 1$ and the zero point (low temperature) approximation applies,

$$(28) \quad \ln(f_c'/f_g)_B = B/T = (1/2)(hc/kT) \sum [(v_{i,c}' - v_{i,c}) - (v_{i,g}' - v_{i,g})]_{\text{high_freqs}}$$

plus an A group containing the low frequencies, $u_i < 1$, treated in the high temperature approximation

$$(29) \quad A = (1/24)(hc/k)^2 \sum [(v_{i,c}'^2 - v_{i,c}^2) - (v_{i,g}'^2 - v_{i,g}^2)]_{\text{low_freqs}}$$

A is generally positive (necessarily positive if it contains contributions only from lattice modes) and predicts $P' > P$. B results from the shifts in internal force constants on condensation. An increased force constant on condensation (blue shift in the associated frequency) leads in the direction of an increased VPIE, a decreased force constant (red shift) leads in the direction of an inverse VPIE ($P' < P$). The $1/T^2$ dependence of the A term in Eq. (27) means that at low

Table 7. *A* and *B* parameters for fits to [-VCIE] and VPiE for selected molecules (per deuterium substitution^a). $\text{RPFR} = A/T^2 + B/T$

	Virial coefficient IE's			Vapor pressure IE's		
	A_{VCIE/n_D}	B_{VCIE/n_D}	Range (K)	A_{VPiE/n_D}	B_{VPiE/n_D}	Range (K)
CH_4/CD_4	233 ± 40	-2.34 ± 0.21	110/300	258	-2.89	90/120
$\text{C}_2\text{H}_6/\text{C}_2\text{D}_6$	53 ± 23	-0.74 ± 0.08	210/520	140	-2.86	115/200
NH_3/ND_3	2630 ± 124	-5.43 ± 0.34	298/473	5 320	-12.20	218/273
$\text{H}_2\text{O}/\text{D}_2\text{O}$	4277	-6.14	473/723	16 900	-35.20	273/423

n_D = number of D atoms substituted.

^a Van Hook *et al.* [114]).

enough temperature A/T^2 must predominate. The IE will be normal and proportional to $1/T^2$. At intermediate temperature the *B* term, which can be positive, but which more typically is negative, may dominate. This accounts for the widely observed crossover to inverse isotope effects (especially common for the deuterated hydrocarbons). At even higher temperatures both terms decay to zero. Thus, the temperature dependence of VPiE can be complicated.

Virial coefficient and vapor pressure isotope effects compared

Van Hook, Rebelo, and Wolfsberg [114] have rationalized the isotope effects on second virial coefficients in the gas phase (VCIE) analogously to the treatment above for VPiE. It is interesting to compare *A* and *B* parameters of fit to VCIE and VPiE for some deuterated molecules (Table 7).

Representative VPiEs, especially H/D effects. Solvent dependence, chromatographic effects

Figure 8 shows VPiEs per D for a few organic compounds and water and ammonia. The effects range from 10% per D normal for $\text{H}_2\text{O}/\text{HOD}$ at the freezing point of H_2O , to 1.6% inverse for methyl acetylene at 160 K. The temperature dependences also vary widely. D for H substitution for hydrogen bonded atoms results in large normal VPiEs with large negative temperature coefficients. This is a consequence of very large blue shifts in the hydrogen bonded lattice modes on con-

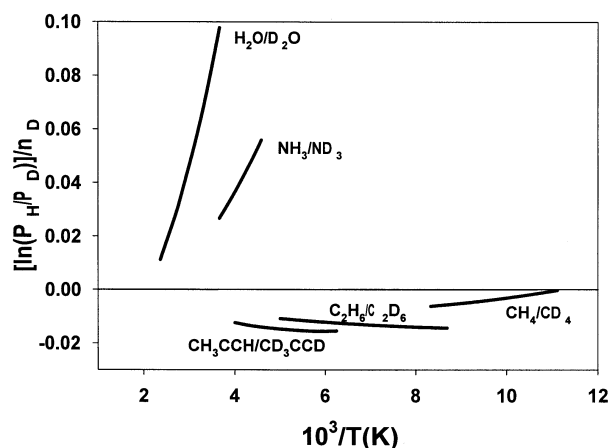


Fig. 8. H/D vapor pressure isotope effects (per atom D) for some compounds.

densation which significantly outweigh the partially compensatory red shift in internal modes. For example for water there is a net red shift of $\sim 280 \text{ cm}^{-1}$ for the internal OH stretching modes but that is more than compensated by the appearance of three blue shifted librational modes (each in excess of 500 cm^{-1}) and three hindered translations. D for H substitution at nonpolar groups like methyl or methylene is different. It is characterized by red shifts in the internal stretching modes caused by the dispersion forces operative in the condensed phase which, although small outweigh the even smaller contributions of the hindered lattice modes. As a consequence H/D VPiEs for nonbonded hydrocarbons are on the order of 1 percent or so inverse per D substitution.

Since VPiE is determined by condensed phase intermolecular forces significant changes should occur when one varies the condensed phase environment. This was nicely illustrated by Dutta-Choudhury, Miljevic and Van Hook [28] who compared the VPiEs for $\text{H}_2\text{O}/\text{D}_2\text{O}$ for the neat liquids (13.1% at 306 K) with those at infinite dilution in benzene (C_6H_6) (-1.4%). The difference is consequent to large changes in both internal and lattice frequencies on transfer from the hydrogen bonded to the nonpolar medium. The VPiE at infinite dilution corresponds to the IE on Henry's Law constants. For the benzenes the change in VPiE on transfer of C_6H_6 or C_6D_6 from the neat liquids (-2.7%) to infinite dilution in H_2O (6.1%) or D_2O (4.0%) also reflects significant frequency changes. Wolff and Hoepfner [124] studied the concentration dependence of the VPiE for $\text{C}_2\text{H}_5\text{NH}_2/\text{C}_2\text{H}_5\text{ND}_2$ dissolved in n-butane. The IEs fall smoothly from large normal effects with large temperature coefficients at $x(\text{amine}) = 1$ to modest inverse effects at $x(\text{amine}) = 0$ (Fig. 9). The behavior is that expected as the strong hydrogen bonds of the amines are broken on dilution with butane (Hoepfner [47]). Another way to measure isotope effects on Henry's Law constants is by using gas or liquid chromatography and a substantial literature reporting such measurements and their interpretation exists (Wolfsberg *et al.* [126], Van Hook [112], Maciej and Thornton *et al.* [71]), but space does not permit further discussion here.

Anharmonic corrections

It is no surprise that harmonic oscillator rigid rotor calculations of VPiEs only agree with experiment over narrow temperature ranges because the harmonic model does not account for thermal expansion of the lattice. These effects are treated empirically by intro-

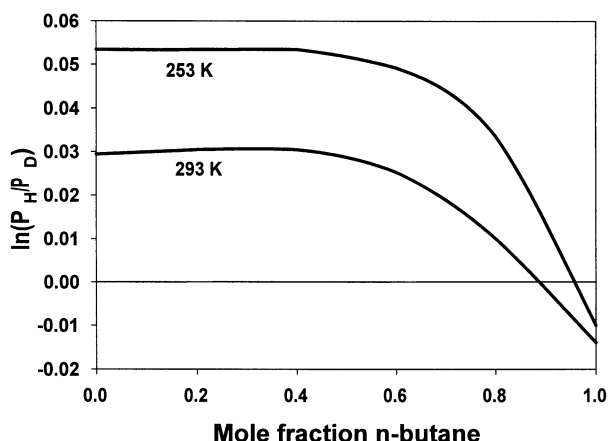


Fig. 9. The vapor pressure ratio $P(\text{C}_2\text{H}_5\text{NH}_2)/P(\text{C}_2\text{H}_5\text{ND}_2)$ in n-butane at two temperatures (Wolff and Hoepfner [124]).

ducing volume dependent best fit lattice frequencies (Gruneisen [38], Van Hook [109]). In this, the Gruneisen or pseudoharmonic approximation, one introduces a set of constants, $\Gamma_i = -(d\ln\nu_i/d\ln V)_T = -(1/2) d\ln(f_i)/d\ln V$. Γ_i is the Gruneisen constant for ν_i , and f_i is the harmonic force constant. Also, $\Gamma_i = -d\ln\nu_i/d\ln V = -(d\ln\nu_i/dP)(dP/d\ln V) = (d\ln\nu_i/dP)/\kappa$ with κ the isothermal compressibility, $\kappa = -(d\ln V/dP)_T$. This relation is useful because there is much more experimental information available on the pressure dependence of vibrational frequencies than on their volume dependence. For lattice translational modes Gruneisen suggested $\Gamma_{tr} = \alpha V/(\kappa C_V)$. Here α is the coefficient of thermal expansion, $\alpha = (\partial\ln V/\partial T)_p$. Typically Γ_{tr} is about 2. For rotation/libration modes and internal vibrations, however, Γ_i is significantly different from 2, for internal modes very much different (much smaller). In the pseudoharmonic formalism the temperature dependences of the various normal mode frequencies arise only indirectly, i.e. through the temperature dependence of the volume. Anharmonic corrections for lattice modes can be important. For example in the ethylene/deuteroethylene system (Bigeleisen *et al.* [13]) it was found the lattice translational and rotational force constants decreased ~ 15 and 40% respectively between 104 and 180 K. One finds that changes in the volume dependent pseudoharmonic internal force constants are relatively much smaller than are the changes in lattice force constants (the internal modes are stiffer and much less sensitive to intermolecular coupling). For ethylene/deuteroethylene the CH stretching constant decreases only 0.15% between 104 and 180 K, bending force constants change about 2% over that temperature range.

It is interesting to compare the empirical pseudoharmonic corrections to VPIE described above with theoretically based and more exact zero point anharmonic corrections for high frequency internal modes (Wolfsberg [125]). Unfortunately this is possible only for those relatively few diatomic and polyatomic isotopomer pairs for which complete vibrational analysis has yielded both harmonic frequencies and first-order (and very rarely second-order) anharmonic contributions to ZPE (Jancso and Van Hook [60]). Jancso, Jakli and Fetzer [55] and Jakli, Juhasz and Jancso [51] used VPIE data for the $\text{CHCl}_3/\text{CDCl}_3$ and $\text{CHBr}_3/\text{CDBr}_3$ pairs to conclude that the anharmonic constants for the CH(D) stretching mode change by about 4% on

condensation (about -4% for CHCl_3 and 4.6% for CHBr_3) at room temperature. Uncertainties in these estimates, $(\delta X^* = -2.6 \pm 0.6 \text{ cm}^{-1})_{\text{VPIE}}$ for CHCl_3 , are less than the uncertainties in the spectroscopic values $(-1.3 \pm 2 \text{ cm}^{-1})_{\text{SPEC}}$. The results indicate that intermolecular forces in liquid chloroform make the CH stretch for this molecule more nearly harmonic than in the vapor, less harmonic for bromoform. Even so we emphasize that vibrational analysis for the vast majority of polyatomics has been limited to the harmonic approximation, and RPIE for these molecules must be calculated using effective harmonic oscillator frequencies and frequency shifts on condensation. (However, it is now possible to use standard quantum chemistry packages to estimate anharmonic corrections to ZPE's and RPIE's).

The dielectric correction

A complication occurs when comparing thermodynamically observed and spectroscopically calculated RPIE's. For high intensity spectroscopic bands shape corrections for the effects of intermolecular interaction are substantial. In the spectroscopic literature they are referred to as "dielectric corrections". For IR intense bands they can amount to 10 cm^{-1} or more and their neglect can lead to large errors in RPIE's derived from spectroscopic measurements (Jancso and Van Hook [59], Maessen and Wolfsberg [72]).

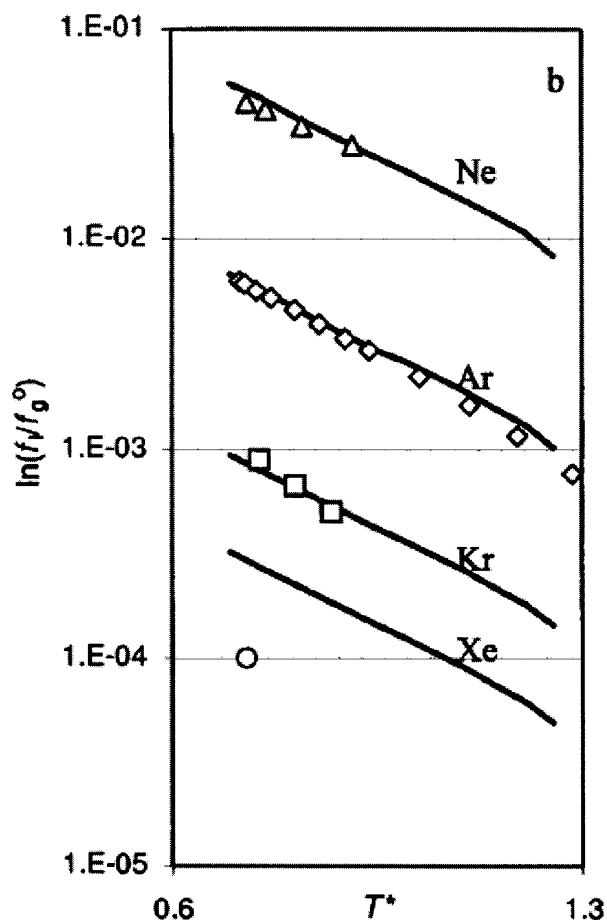


Fig. 10. Theory (lines) and experiment compared for VPIE's of rare gases. [$T^* = kT/\epsilon \sim 1.30 T/T_{\text{critical}}$ with ϵ the Lennard-Jones well depth] (Lopes *et al.* [69]).

A few examples of VPIEs

(a) Rare gases

Precise intermolecular potentials are available for monatomic He, Ne, Ar and Xe. This permits accurate calculations of the VPIE's of these gases, their mixtures, and rare gas isotopomer mixtures. Figure 10 compares calculated RPF's with experiment (Lopes *et al.* [69]). The input parameters (well depth, ϵ , and size parameter, σ) for each species are completely defined in terms of the observed critical properties for each of the fluids. The agreement with experiment is remarkably good, especially considering that the VPIE's span several orders of magnitude. Although the LJ potential is only approximate, it turns out to be an excellent choice to represent IE's in rare gas systems. The thermodynamic properties are described with a single master (reduced) equation. Theory and experiment are in satisfactory agreement.

(b) Ethylene isotopomers

Vapor pressures of C_2DH_3 , *cis*-, *trans*-, and *gem*- $C_2D_2H_2$, C_2D_3H and C_2D_4 , and $^{12}C^{13}CH_4$, have been measured at high precision and theoretically interpreted (Bigeleisen

et al. [13]). VPIE's for the liquids are inverse, but there is a large positive discontinuity on freezing. Ethylene was one of the first systems subjected to detailed vibrational analysis. Agreement with experiment is excellent (Fig. 11). A single isotope independent force field suffices to fit the experimental data for all seven isotopomers over a wide temperature range. The differences in the VPIE's of the equivalent isotopomers *cis*-, *trans*-, and *gem*-dideuteroethylene demonstrate the close connection between molecular structure and isotope chemistry. The IE's are mainly a consequence of hindered rotation in the liquid (moments of inertia for *cis*-, *trans*-, and *gem*- $C_2D_2H_2$ are slightly different), but superposed on that effect is an additional ZPE contribution caused by coupling between the hindered rotational modes in the liquid and certain internal vibrations.

(c) Benzene isotope effects

VPIE's for C_6H_5D , *ortho*-, *meta*-, and *para*- $C_6H_4D_2$ and C_6D_6 are available between the normal melting and boiling points, as are data on the excess free energy of mixing (small and positive) for C_6H_6/C_6D_6 , the $^{13}C/^{12}C$ effect at the boiling temperature, VPIE's and MVIE's (molar volume isotope effects) for C_6H_6/C_6D_6 across the entire LV coexistence range, triple to critical points, and

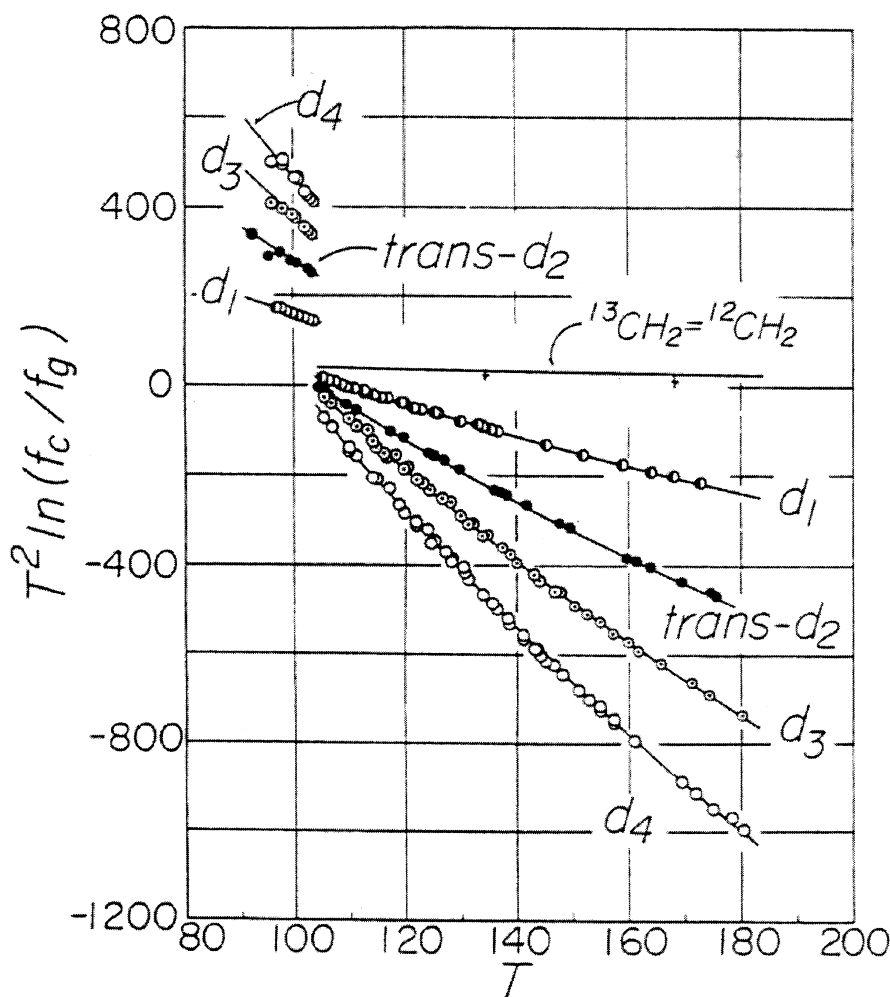


Fig. 11. Plot of $T^2 \ln(f_c/f_g) = T^2 \ln(f_c/f_g)$ for isotopically substituted ethylenes. The lines are calculated from an isotope independent force field (Bigeleisen *et al.* [13]).

isothermal compressibility IE's between 288 and 313 K (Jakli *et al.* [52], Kooner and Van Hook [66], Matsuo and Van Hook [74]). HOVM calculations show good agreement with spectroscopic information and reproduce the observed subtle deviations from the law of the mean in the series D₁, D₂,..., D₆, and the VPIE's between equivalent isomers *ortho*-, *meta*-, and *para*-C₆H₄D₂ (Jancso and Van Hook [61]). With (df_{CH}/dV) obtained from VPIE of one isotopomer pair, and using the experimentally observed molar volume isotope effect, one calculates $\mu^E = 1.8$ J/mol for the excess free energy of isotopomer mixing in the low temperature fluid in good agreement with experiment, 2.1 ± 0.3 J/mol. The agreement furnishes strong support for the theoretical development correlating molar volume isotope effects and excess free energies of solutions of isotopomers (following section).

Excess free energies in isotopomer solutions

Jancso, Rebelo and Van Hook [56, 57] have reviewed vapor pressure data on solutions of mixtures of isotopes (³⁶A/⁴⁰Ar, HCl/DCl, C₆H₆/C₆D₆, polystyrene-h/d, etc.) which definitively show small but significant deviations from the behavior of ideal solutions (i.e. show excess thermodynamic properties of solution). An excess thermodynamic property is just the difference between the value of that property for the real (nonideal) solution and the corresponding ideal solution. The pseudo-harmonic cell model leads straightforwardly to the idea that the excess free energies of isotopomer mixtures correlate with the isotope effect on the molar volumes of the pure isotopomers (MVIE's). One calculates the free energy of mixing in a two step process: (1) compress or dilate each separated component to the molar volume of the solution, and (2) mix at constant volume, assuming the free energy change in step (2) is zero. In terms of the harmonic oscillator cell model the change in the Helmholtz free energy, A , in the first step is

$$(30) \quad -RT \ln(\gamma) = -\int (dA/dV)dV \\ = -RT \int \sum [(d \ln(Q_i)/dv_i)(dv_i/dV)dV]_{3n_{\text{freqs}}}$$

The integral is from V to V' . With Eq. (30) the contributions of internal modes are properly evaluated. Also apparent differences between RPFH obtained via VPIE or LVFF can be successfully rationalized (see Eqs. (23) and (25)), and the excess free energies in concentrated solutions of isotopomers, one in the other, interpreted. Examples are given in Table 8.

Table 8. Excess free energies of some isotopomer solutions

System	T (K)	x'	$10^4 \ln \gamma^a$	G^E /(J/mol)
³⁶ Ar/ ⁴⁰ Ar	84	0	-3	0.015
	90	0.5		
CH ₄ /CD ₄	100	0.5		0.57
HCl/DCl	170	0.5		0.66
H ₂ S/D ₂ S	190	0.5		-0.92
C ₆ H ₆ /C ₆ D ₆	298	0.5		0.58
c-C ₆ H ₁₂ /c-C ₆ D ₁₂	298	0.5		1.08
Polybutadiene-h/-d	296		9	

^a Activity coefficient of the more dilute species.

Phase separation of isotopomer solutions

Phase separation is a straightforward consequence of solution nonideality. In regular solution theory the total excess free energy is expressed, $G^E = x'\mu'^E + x\mu^E = xx'\chi$. In first approximation the Flory-Huggins parameter χ is independent of temperature and concentration, and the thermodynamic conditions for the initial liquid-liquid phase separation from symmetrical mixtures are $x = x' = 0.5$ and $\chi/RT = 2$. For $\chi/RT > 2$ there is incomplete mixing, i.e. phase separation. Typically, IE's on the excess free energy, now expressed in terms of the parameter χ , are inversely proportional to the temperature raised to some power, and directly proportional to the total isotope and phase frequency shift, $\Delta\delta\nu$. It follows that liquid-liquid demixing of isotopomers will be enhanced at very low temperature, or, should one be restricted to higher temperature because the solution freezes, to molecules with very many (isotopically substituted) oscillators. The first case is realized for ³He/⁴He and H₂/D₂ mixtures, the second by polymer/polymer mixtures. It is long known that ³He/⁴He liquid mixtures phase separate at temperature below 0.9 K. The theoretical explanation, first advanced by Prigogine, has been outlined above. Similarly, mixtures of solid ³He/⁴He (formed at elevated pressure) and mixtures of solid H₂/D₂ phase separate, but liquid mixtures of H₂ and D₂ do not, although they do show appreciable nonideality. No other "small molecule" isotopomer mixtures phase separate. In polymers, however, while the excess free energy per oscillator is small, the effects are cumulative, and as the number of isotopically substituted bonds increases the excess free energy becomes large enough to cause phase separation in binary mixtures of perprotio and perdeutero polymers. This occurs at the critical polymerization number N_{critical} where $\chi/RT = 2$. Phase separation has been observed in polystyrene(H/D), polybutadiene(H/D), and polyethylene-polypropylene(H/D) mixtures. For polybutadiene the number of CH/CD substituted bonds per monomer unit is 6, and the critical polymerization number for H/D demixing is 1.2×10^3 monomer units (Singh and Van Hook [93], Bates and Wilthuis [7]).

Demixing of small molecule and polymer-solvent solutions

Both polymer-solvent and small molecule demixing diagrams may show upper and lower consolute branches which are functions of temperature, chain length, con-

centration, pressure, and H/D substitution (Imre and Van Hook [49]). The two branches may approach each other as some other variable (polymerization number, isotope fraction, or pressure, for example increases) and can join at a double critical (hypercritical) point. Detailed investigation of demixing as a function of these variables has been reported by groups in Tennessee, Warsaw, Budapest and Lisbon (see for e.g. Van Hook [111], Imre and Van Hook [49], Visak, Rebelo and Szydowski [118]). Isotope effects in these systems are large. For example, in acetone-h the hypercritical MW for polystyrene is $\sim 22,000$ at $P = 0.1$ MPa, but in acetone-d the hypercritical MW has dropped to 13,500 (i.e. $\ln[MW_{yD=0}/MW_{yD=1}] = 0.49$ which is a remarkably large IE; deuteration operates in the same direction as a drop in pressure, i.e. a decrease in solvent quality). At constant MW and $P = 0.1$ MPa the solvent IEs are also large, for example $\ln(T_{UCST}/T_{UCST})_{13,500} \sim -0.22$ and $\ln(T_{UCST}/T_{UCST})_{7500} \sim -0.09$ (UCST = upper critical solution temperature). The effect of hypercritical enhancement is obvious.

Another interesting example: critical demixing loci of small molecule solutions of 3-methylpyridine (3-MP) in H_2O/D_2O solvents are shown in $T, P, x(3-MP)$ space, Fig. 12 (Visak *et al.* [118]). At atmospheric pressure a 70 K closed immiscibility loop, ($T_{UCST} - T_{LCST}$), is observed for (3-methylpyridine + D_2O) and the immiscibility gap is modestly pressure dependent. In the (p,T) projection the phase diagram shows a characteristic “hour-glass” shape. On addition of H_2O the gap shrinks, becomes more and more pinched at the waist, and at 21 wt.% D_2O it disappears completely as the phase diagram changes from this “hour-glass” to a shape that resembles the UCST/LCST configuration in the (T,x)

plane – two immiscible domes, an upper and a lower. With continued addition of H_2O , holding (3-methylpyridine + water) at the critical concentration, the upper and lower immiscible branches move further and further apart, until finally at high enough H_2O/D_2O (17 wt.% D_2O) the low-pressure branch is no longer present at atmospheric pressure, dropping below the $P = 0$ isobar. For (3-methylpyridine + H_2O) the miscibility gap between the upper and lower branches amounts to ~ 160 MPa. The phenomenon corresponds to an impressive pressure shift of hundreds of atmospheres merely upon (H/D) solvent isotope substitution. Very large isotope effects like these seem to be limited to the hypercritical regions of phase diagrams, i.e. not too far from thermodynamic divergences of the type $(dP/dT)_c = \infty$ or $(dT/dP)_c = \infty$.

Other solubility IE studies

Scharlin and Battino [89, 90] have reviewed gas solubility IE's in H_2O and D_2O . Rabinovich [83] reports solubilities of H_2 and D_2 in various solvents, and has also compiled solvent IE data (H_2O/D_2O) for numerous ionic electrolyte solutions.

Isotope effects on some other molecular properties

Dipole moments, polarizabilities

Rabinovich [83] and Wolfsberg *et al.* [126] have reviewed data on dipole moment and polarizability isotope effects. The effects are small. Polarizability IEs are most conveniently measured using differential refrac-

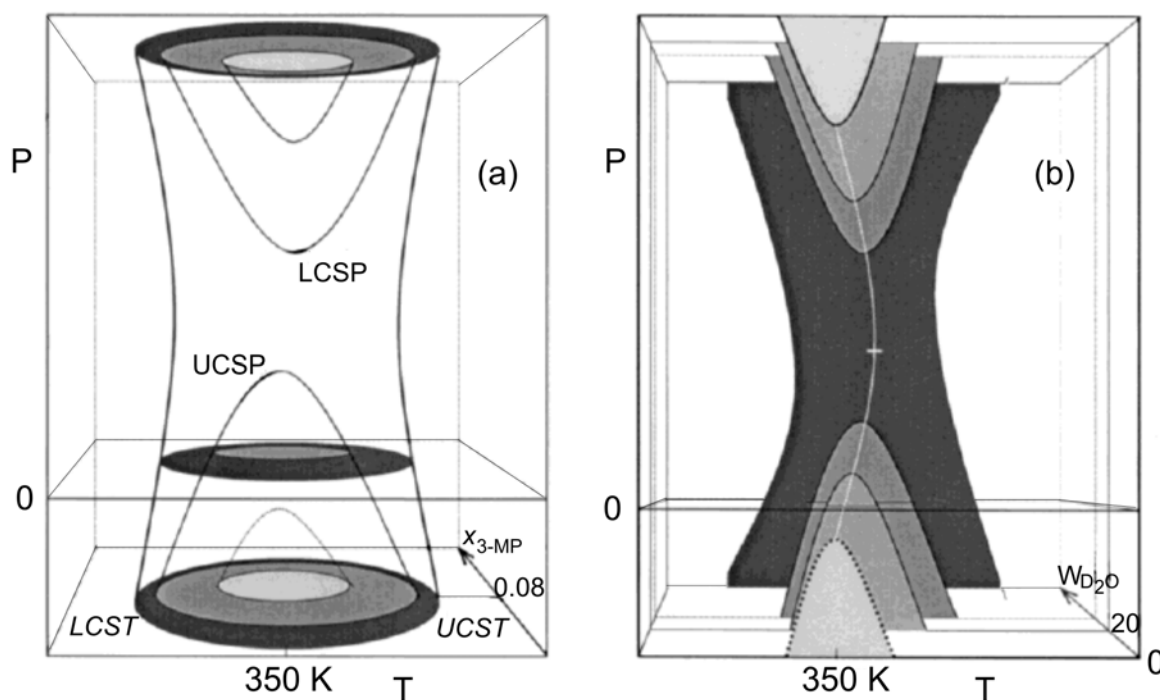


Fig. 12. Two representations of the phase diagram for 3-methylpyridine/water(H/D). (a) T - P - $x(3-MP)$ for three different H_2O/D_2O concentration ratios. The inner ellipse and corresponding critical curves hold for $(0 < W(D_2O)/wt.\% < 17)$. The intermediate ellipse is for $(17 < W(D_2O)/wt.\% < 21)$, and the outer $(21 < W(D_2O)/wt.\% < 100)$; (b) Phase diagram at approximately constant critical concentration 3-MP ($x \sim 0.08$) showing the evolution of the diagram as the deuterium content of the solvent varies (Visak *et al.* [118]).

tometry and Urbanczyk and Van Hook [102, 103] and Wiczorek, Urbanczyk and Van Hook [121] describe a continuous dilution differential refractometric technique to measure isotopic refractive index differences, refractive indices, and excess volumes for solutions of isotopomers. The dipole moment and polarizability express the first and second order interactions of a molecule with an impressed electric field. Isotope effects on these electronic properties are a consequence of isotopic differences in vibrational anharmonicity. Van Hook and Wolfsberg [116] have discussed the theoretical origin of the effects and correlated polarizability and molar volume IEs. Many years ago Bell and Coop [8] advanced the idea that the IE on dipole moment, $\Delta\mu$, for diatomic molecules is given by the product of the difference averaged bond lengths and the dipole moment derivative. In the diatomic case, (HCl/DCl for example), one obtains

$$(31) \quad \Delta\mu = \mu_{\text{H}} - \mu_{\text{D}} = (\partial\mu/\partial r)_e (\langle r_{\text{H}} \rangle - \langle r_{\text{D}} \rangle)$$

It is well established that the average lengths of CH bonds are consistently 0.003 to 0.004 Å longer than the corresponding CD bonds in the ground vibrational state due to anharmonic effects. The dipole moment derivative, $(\partial\mu/\partial r)$, at the equilibrium bond length is available from theoretical calculation or spectroscopic measurement (via precise measurements of IR intensities of vibration-rotation bands). Calculations based on Eq. (31) yield predicted dipole moment IE's in reasonable agreement with experiment.

Isotope effects on NMR shielding

An enormous literature dealing with isotope effects on NMR parameters has accumulated over the years including studies on chemical shift and coupling constant IE's, the use of isotope labeling for molecular structure determinations, the study of fast exchange processes, and the use of NMR as an analytical tool to measure isotope fractionation (Diehl *et al.* [27], Hansen [39]). Our attention is limited to IE's on chemical shifts (nuclear shielding) due to isotopic differences in averaging of rotation-vibration contributions to molecular properties (rovibrational effects). The theory described by Jameson [53] points out the isotope effect on shielding (σ) depends on vibrationally averaged bond lengths and angles (different due to anharmonic effects) weighted by a set of isotope independent shielding parameters $(\partial\sigma/\partial r_i)$, $(\partial^2\sigma/(\partial r_i \partial r_j))$, $(\partial\sigma/\partial\alpha_{ij})$, etc. which are most reliably obtained from *ab initio* quantum mechanical calculation. An excellent illustration of the application of rovibrational theory to NMR shift data, including comparison with experiment is given in Table 9. The agreement is reasonable although the calculated values are consis-

tently about 20% larger than experiment, probably because the bond length dependence of nuclear shielding, $(\partial\sigma/\partial r_i)$, is overestimated by the choice of Hartree-Fock wave functions used in the calculation.

Molar volume isotope effects

Molar volume isotope effects (MVIE's) for common liquids between the triple and boiling points amount to a few parts per thousand or less per H/D substitution. At temperatures well below the critical point liquid molar volumes generally lie within 10% or so of the values for the solids at the triple point and it is reasonable to assume a model where liquid state molecules, on average, are in contact with one another. For convenience this approach is called "the mechanical model". At higher temperatures the expansivity and compressibility increase rapidly, the liquid expands dramatically (typically critical volumes are some 3 or 4 times molar volumes at T_{TRP}), and the mechanical model is inappropriate. Except for $^3\text{He}/^4\text{He}$ MVIE data are only available for H/D substituted molecules, because the effects for heavier isotopomer pairs are too small to be conveniently measured. Both positive and negative effects are observed for low temperature liquids, but negative values (i.e. $V_{\text{D}} > V_{\text{H}}$) only occur for strongly associated (hydrogen bonded) liquids. MVIEs are well known for (CH_4/CD_4 , $\text{C}_6\text{H}_6/\text{C}_6\text{D}_6$, and $\text{H}_2\text{O}/\text{D}_2\text{O}$) between T_{TRP} and T_{critical} . In each case MVIE is relatively flat at low temperature (i.e. $\partial(\ln(V'/V))/\partial T \sim 0$ for $(\sim 0.45 < T/T_{\text{critical}} < \sim 0.6)$) but at higher temperature it drops off rapidly and reaches large negative values. MVIE's for $^3\text{He}/^4\text{He}$ and H_2/D_2 , on the other hand, are large and positive (hundreds of parts per thousand) and increase rapidly with temperature. At these higher temperatures MVIEs are best treated with corresponding states theory (Van Hook, Rebelo, Wolfsberg [115]). The discussion here is concerned with the application of the mechanical model to H/D effects at lower temperatures. That model, introduced by Bartell and Roskos [6], assumes that the major part of MVIE for polyatomic molecules at low temperature is due to the isotope effect on the XH/XD vibrational amplitudes. For example, for $\text{C}_6\text{H}_6/\text{C}_6\text{D}_6$ taking the IE on CH/CD vibrational amplitude as 0.005 Å, one finds (modeling benzene as a disk) $\Delta V/V = 2\Delta r/r = 2(0.005)/3.7 = 0.0027$, in reasonable agreement with the observed value, 0.0021. Here 3.7 Å is the Van der Waals radius of benzene. Similarly for CH_4/CD_4 , $\Delta V/V = 3\Delta r/r = 3(0.005)/(2.3) = 0.007$ (observed = 0.011). The predicted MVIE's are in rough agreement with observation, but the model is crude and needs refinement. It is unable to predict the temperature coefficient of the MVIEs of non-polar molecules and it is not applicable to complicated liquids, for example ones with hydrogen bonded networks like water. For

Table 9. Calculated^a and observed^b IE's on carbon-13 shielding constants of methane isotopomers at 300 K, $-\langle\sigma'\rangle - \langle\sigma\rangle$ (in ppm)

$\langle\sigma\rangle$	$^{13}\text{CH}_3\text{D}$	$^{13}\text{CH}_2\text{D}_2$	$^{13}\text{CHD}_3$	$^{13}\text{CD}_4$
Calculated	0.250	0.500	0.746	0.992
Experiment	0.187	0.385	0.579	0.774

^a Raynes *et al.* [84].

^b Alei and Wagman [1].

$\text{H}_2\text{O}/\text{D}_2\text{O}$ the MVIE is inverse and shows a complicated temperature dependence connected with IEs on the amplitudes of the external librational modes and the gradual loss of the hydrogen bonded structure with increasing temperature. The librational motions occur about the center of mass which is isotope dependent for these non-centrosymmetric molecules and this accounts for the anomalous behavior (Dutta-Choudhury and Van Hook [29], Wolfsberg *et al.* [126]).

Corresponding states and IEs: critical property IEs

In spite of the success of corresponding states (CS) theory in describing the PVT properties of fluids, it has been rarely applied to the interpretation of IEs. In CS the temperature dependence of the molar volume and the conditions for liquid-vapor coexistence are expressed using the critical properties of the fluid and one or more additional parameters. In applying CS to isotope effects, quantization, essential to the understanding of thermodynamic IE's, is introduced in terms of the critical property IE's. CS ignores the subtleties of molecular structure and vibrational properties and therefore cannot be expected to be as useful for rationalization of vapor pressure IE's as it is for molar volume IE's. The VPIE depends on subtle isotopic differences in the vibrational properties of the coexisting vapor and liquid phases. The molar density IE, on the other hand, is a much simpler function of the molecular structure and overall motion in the condensed phase. Corresponding states fits to vapor pressure IE's are not as good as those to

molar volume IE's, even after the empirical introduction of an additional isotope dependent parameter. Van Hook, Rebelo, and Wolfsberg [115] recently described a modified Van der Waals corresponding states equation which yielded useful representations of VPIEs and MVIEs over the complete liquid range, T_{TRP} to T_{critical} . They also developed correlations of critical property IEs with each other and near critical values of the VPIE (Fig. 13). This permits the estimation of the IEs, $\Delta T_{\text{critical}}/T_{\text{critical}}$, $\Delta V_{\text{critical}}/V_{\text{critical}}$, and $\Delta P_{\text{critical}}/P_{\text{critical}}$ from the critical temperature of the more common isotopomer, T_{critical} , and a near critical value of VPIE. That information in hand, the corresponding states equation yields $\ln(V'/V)$ across the entire liquid coexistence range. This is a very useful result: few data are available for MVIEs except near room temperature, and experimental programs to expand the data base are difficult, expensive, and tedious to implement. Corresponding states analysis offers an attractive alternative.

IEs in geochemical and environmental studies

Measurements of the isotope ratios of naturally occurring materials have long provided important information in geochemistry, meteorology, evolutionary biology, and archeology. For example, comparisons of isotope distributions in coexisting minerals, with those measured in the laboratory, or with theoretically calculated ratios, have been used to specify the conditions of formation of the mineral. Similarly, fractionation of the hydrogen and oxygen isotopes of

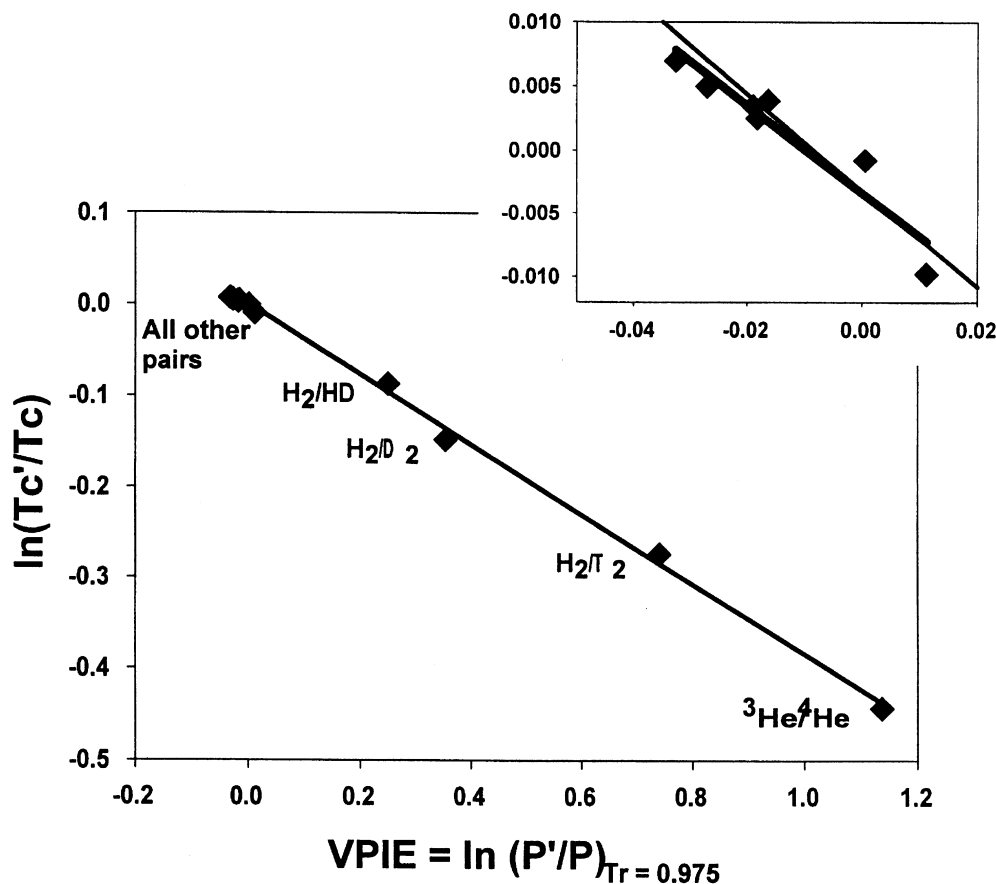


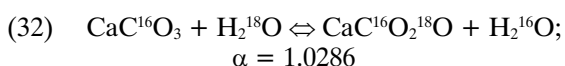
Fig. 13. The correlation of $\ln(T_c'/T_c)$ with $\ln(P'/P)$ at $T_r = T/T_c = 0.975$ (Van Hook *et al.* [115]).

water during natural phase changes (i.e. evaporation, rain, snow, or ice formation), or chemical changes (precipitation of hydrated minerals, biological/metabolic equilibration, etc.), furnish information on the nature of those processes. Such information can be difficult to obtain because one is interested in small changes, say a percent or so, in the natural abundance ratio which is typically small itself. For example the oxygen isotope ratio in natural waters, $R = {}^{18}\text{O}/{}^{16}\text{O}$, normally lies in the range ($0.0019 < R < 0.0021$). Thus a 1% ${}^{18}\text{O}/{}^{16}\text{O}$ IE characterizing some physical or chemical change of interest amounts to a change of about $\Delta R = 0.00200 \times 1.01 - 0.00200 = 0.00002$, i.e. 20 ppm (parts per million). For D/H, $R = 1.58 \times 10^{-4}$ and a 1% effect amounts to only $\Delta R = 1.6$ ppm. These are small changes indeed and careful attention to experimental detail and sophisticated instrumentation are required to assure sufficient precision and accuracy to distinguish between alternate explanations for observed fractionations. High precision isotope ratio mass spectrometry is the technique of choice for measurements of geochemical and environmental IEs. Criss [25], Galimov [33], Hoefs [46], and Richardson and McSween [85] afford entry points into the literature.

Unfortunately space permits only a cursory glance at several examples of geochemical interest.

Geochemical temperature scales

In the late 1940's H. C. Urey recognized that the temperature dependence of the isotope exchange equilibrium between water and calcite (the principal mineral in marine limestones) could be employed as a paleo-thermometer. At 298.15 K the fractionation factor for calcite-water is 1.0286,



which is to say $\delta^{18}\text{O} = 1000(\alpha - 1) = +28.6$, provided the calcite was laid down from standard ocean water. Since the temperature dependence of α was known ($d\alpha/dT \sim -0.23 \text{ o/oo K}^{-1}$), accurate $\delta^{18}\text{O}$ measurements on ancient marine sediments could be used to determine water temperature at the time the sediment was precipitated. Details were reported in 1951 (Urey *et al.* [105]). In addition to presupposing development of instrumentation of the necessary precision, the method depended on two important assumptions: (1) the isotope concentration of the ocean has remained constant over time and position; (2) the mineral was deposited in thermodynamic equilibrium with ocean water, and has remained unchanged over long periods of time. The carbonate paleo-temperature scale has aided our understanding of the climate changes Earth has experienced during the last ~ 3 million years, a period of intermittent glaciation. A prime criticism of the $\delta^{18}\text{O}$ carbonate paleo-temperature scale is the absence of any independent measure of the isotopic composition in ancient seawater. Therefore isotopic fluctuations in the sediments do not necessarily correlate with changes in temperature alone. Even so, the basic idea remains valid.

Many ore deposits contain coexisting mineral pairs which have been formed in equilibrium as judged by independent (non-isotopic) criteria. In such cases the mineral-mineral fractionation values for a given M-N mineral pair, $\Delta = \delta_N - \delta_M$, correlate straightforwardly with the geochemical temperature of mineral formation (it being supposed that the equilibrium is "locked-in" as temperature rapidly falls after the initial ore formation). At the high temperatures of formation of metamorphic or igneous rock deposits the isotope fractionation for many mineral systems closely follows the $1/T^2$ dependence predicted by the high temperature approximation to equilibrium isotope fractionation.

Isotope hydrology

Large changes in the isotope signature of water are associated with condensation, evaporation, or melting. At equilibrium the fractionation between two coexisting phases is a function of the temperature. When water evaporates from the ocean it shows $\delta\text{D} \sim -80 \text{ o/oo}$ and $\delta^{18}\text{O} \sim -9 \text{ o/oo}$, less (i.e. more negative) at high latitudes, more (less negative) at lower latitude. No matter the location, however, atmospheric water vapor always has negative δD and $\delta^{18}\text{O}$ relative to standard mean ocean water (SMOW) because the vapor pressure of H_2^{16}O is greater than those of HD^{16}O or H_2^{18}O at all temperatures of meteorological interest. Fractionation data are usually displayed using a three isotope plot (Fig. 14). Meteoric waters lie on or close to the correlation line $\delta\text{D} = 8.2 \delta^{18}\text{O} + 10.4$. Shallow ground-waters follow the same pattern, but waters from deep aquifers, geothermal waters, ice cores, etc. can and do lie well off the line.

Ice cores

The ice sheets of Greenland and Antarctica are several kilometers thick and preserve a sequential record of high latitude precipitation over tens of thousands of years. This record has been studied by the deep core Arctic and Antarctic drilling programs during the past thirty or more years. The "Vostok" core drilled in the high Antarctic through ~ 3.7 km of ice sampled fossil ice as old as $\sim 350,000$ years. The Vostok data show several sharp saw-toothed climatic cycles. The ice samples

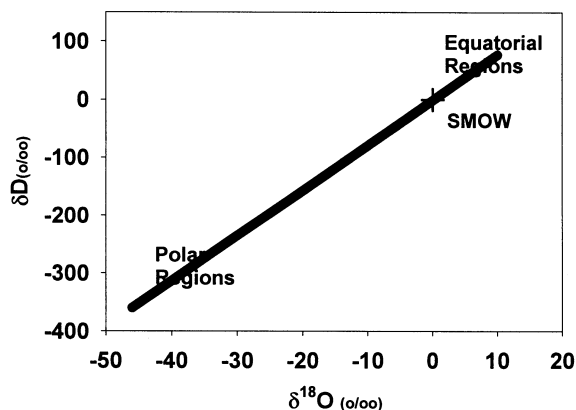


Fig. 14. Three isotope plot showing $\delta^{18}\text{O}$ and δD values for meteoric waters (Wolfsberg *et al.* [126]).

corresponding to the maxima are lower than modern precipitation at this location by $\delta D = \sim 50$ ‰ and $\delta^{18}O = 6$ ‰ suggesting that average temperatures during those periods of glaciation were about 10 K lower than present day ones. It is interesting that the pattern of the ice core data reflects that of the tropical sedimentary carbonate cores. The $\delta^{18}O$ saw-tooth pattern occurs at the same intervals, but has smaller amplitude and is of opposite sign. The cycles represent a combination of the effects of climate change and changes in $\delta^{18}O$ in seawater caused by the growth or retreat of the polar ice caps (Shakleton *et al.* [91]).

Paleo-diets

As a final example in this section we consider the application of geochemical isotope techniques to diet. The complex biochemical paths in organisms offer many ways to fractionate isotopes by both kinetic and equilibrium processes. It is therefore expected, and it is observed, that the different carbon, hydrogen, oxygen and nitrogen atoms in organic residues show compound and atom-site specific isotope fractionations (Galimov [33]). A thoroughly studied example that of the several different pathways of photosynthetic carbon fixation by plants. Terrestrial plants using C_3 (e.g. rice, wheat, beets, potatoes, legumes) and C_4 (e.g. maize, corn, sorghum, sugar cane) photosynthetic pathways show different ^{13}C fractionations. The distinction between C_3 and C_4 is in the number of carbon atoms found in the products of the initial metabolic conversion step. C_4 plants such as maize contain relatively large amounts of carbohydrate and protein and typically show $\delta^{13}C \sim -15$ ‰. This compares to the ~ -25 ‰ found in C_3 plants which contain larger amounts of lignin, cellulose and lipids. Marine plants (including plankton) show $^{13}C/^{12}C$ about 8 ‰ lower than C_3 plants, most likely because they fix marine HCO_3^- (0 ‰) rather than atmospheric CO_2 (-7 ‰). Since, roughly, the degree of isotope fractionation in the plants lying at the base of the food chain is expected to carry over to the animals which consume them, it follows that such isotope ratios can be used to study animal (and human) ecology and archeology (“they are what they eat, ± 1 or 2 per mil”). That turns out to be the case. In one interesting study the arrival of maize agriculture from Central America into the lower Illinois valley around 1000 AD was demonstrated by measuring $\delta^{13}C$ of human bone collagen as a function of time. Because of a lack of direct archeological evidence concerning ancient Native American agricultural practice the isotope data helped solve an otherwise intractable problem. This methodology has been widely applied (DeNiro [26]).

Unimolecular processes. The “mass independent” fractionation of ozone

A straightforward consequence of the standard theory of equilibrium isotope effects is that the ratio of ratios of fractionations can be calculated from the differences in mass and mass distribution of the reacting particles, and this is independent of the particulars

of any fractionation process. Thus for a three isotope mixture, for example H, D, T or ^{16}O , ^{17}O , ^{18}O , the equilibrium theory predicts the ratio of concentrations $([D]/[H])/([T]/[H])$ or $([^{17}O]/[^{16}O])/([^{18}O]/[^{16}O])$ to be approximately 0.5. For oxygen isotope effects that line, generally known as the terrestrial fractionation line (TFL), but occasionally as the earth-moon line, has been experimentally established by measurements on many thousands of samples of oxides, silicates, carbonates, etc. from earth and moon and is completely consistent with isotope effect theory. For the three isotope set ^{16}O : ^{17}O : ^{18}O along TFL $\delta^{17}O = m \delta^{18}O$ with $m \sim (1 - 16/17)/(1 - 16/18) = 0.529$. It was therefore highly surprising to discover that oxygen isotope fractionation for certain inclusions found in meteorites did not follow the expected pattern, but unexpectedly showed $([^{17}O]/[^{16}O])/([^{18}O]/[^{16}O]) \sim 1$, i.e. “mass independent fractionation” (Fig. 15). Then current thinking assumed that all possible geophysical and geochemical processes produced mass dependent isotope fractionations ($m \sim 0.53$ for oxygen), and large differences from that value most likely reflected the intervention of some nuclear event. It forced the conclusion that the meteorites had sampled a region where the “primordial soup” was significantly different than for the earth/moon. This conjecture, however, was shown experimentally to be unnecessary by Thiemens and coworkers in the early 1980s (Thiemens and Heidenreich [100], Thiemens [99]) who studied (nonequilibrium) isotope fractionation during the production of ozone from oxygen in an electric discharge. The product ozone was equally enriched in ^{17}O and ^{18}O , so $m \sim 1$, rather than the expected mass dependent value, $m \sim 1/2$. The slope of the mass-independent line is the same for terrestrial ozone synthesis as it is for the meteorite data. This leads to the conclusion that the mass independent slope for the meteorite fractionation might have a chemical rather than a nuclear origin (assuming some plausible mechanism which transfers ozone fractionation from the low pressure gas to Ca/Al oxide inclusions in meteorites).

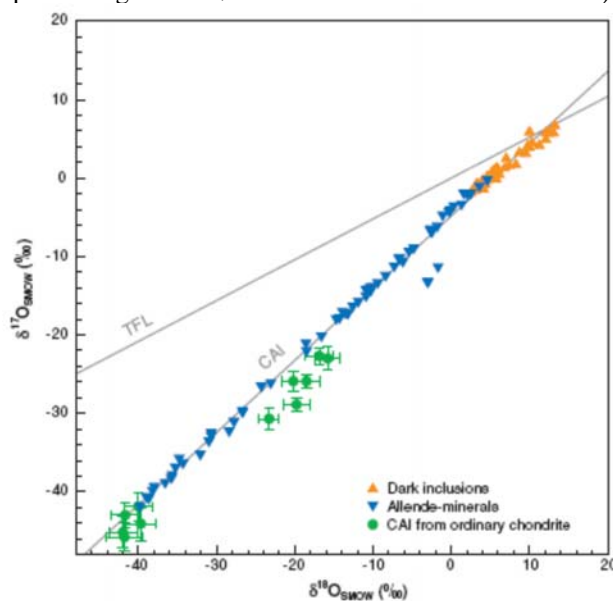


Fig. 15. Three isotope plot of inclusions in chondritic meteorites compared with the terrestrial fractionation TFL line (Thiemens [99]).

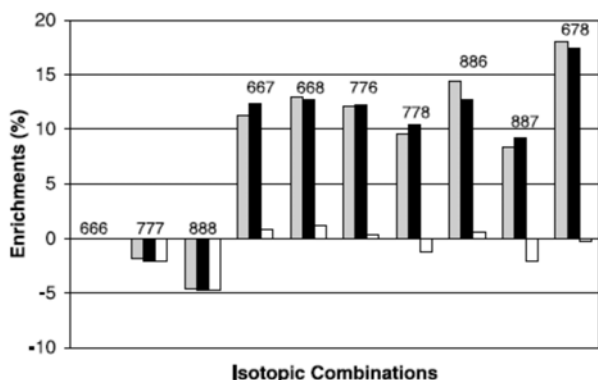


Fig. 16. Experimental and calculated fractionations of ozone isotopomers. The labels 6, 7 and 8 represent ^{16}O , ^{17}O , and ^{18}O respectively. Experiment = gray, calculated = black. The clear bars show calculated values based on a different choice of isotopomer independent parameter (Gao and Marcus [34]).

Also, measurements on natural ozone samples collected at high altitude, far into the stratosphere, show mass independent fractionation, not only for ozone but for other oxygen containing molecules (sulfates, nitrogen oxides, and carbon dioxide). These upper atmosphere fractionations can be transferred from the low pressure gas to aerosol particle surfaces and eventually to precipitated bulk phase solids.

Figure 16 compares measured and calculated isotope fractionations for all ozone isotopomers prepared from an enriched oxygen precursor (Gao and Marcus [34]). In this figure ($^{16}\text{O}^{16}\text{O}^{16}\text{O}$, $^{16}\text{O}^{16}\text{O}^{17}\text{O}$, etc. are represented as; 666, 667, 676, 677, etc.). The calculations are in quantitative agreement with experiment. The pattern shown in Fig. 16 does not vary a great deal with the temperature or pressure at which the synthesis is carried out and is consistent with experiments on natural abundance starting material, and with samples collected from the upper atmosphere. In the calculations Marcus and coworkers applied their modernized version of the RRKM (Rice-Ramsberger-Kassel-Marcus) theory of unimolecular reactions to the ozone problem. They considered a kinetic scheme in which a collisionally activated and short lived intermediate, O_3^\ddagger , ($\text{O}_2 + \text{O} \rightarrow \text{O}_3^\ddagger$) undergoes a rapid series of steps which redistribute its internal and rotational energy, but then at some point may dissociate by one of two available paths, for example $^{16}\text{O}^{16}\text{O}^{18}\text{O}^\ddagger \rightarrow ^{16}\text{O}^{16}\text{O} + ^{18}\text{O}$ or $^{16}\text{O}^{16}\text{O}^{18}\text{O}^\ddagger \rightarrow ^{16}\text{O} + ^{16}\text{O}^{18}\text{O}$, or as a third alternative may collide with bath molecules and deactivate to stable ozone, $^{16}\text{O}^{16}\text{O}^{18}\text{O}^\ddagger + \text{bath} \rightarrow ^{16}\text{O}^{16}\text{O}^{18}\text{O} + \text{bath}$. The rate constants for the three processes for each activated isotopomer species are dependent on the kind and number of vibrational and rotational quantum states characterizing the activated and product species. The calculation of the overall rate of formation for each isotopomer involves integrations of these state specific reaction probabilities weighted by the density of states for both activated species and product. It is important to recognize that in no sense is an equilibrium between activated state and reactants ever established, nor is one ever approached. It is for that reason that ordinary Bigeleisen-Mayer kinetic isotope theory is not applicable to this problem, nor for that matter to unimolecular reactions in general. The calculated isotope enrichments for the different

possible ozone isotopomers are compared with experiment in Fig. 16. The agreement is excellent. The nearly mass independent fractionation observed for the asymmetric isotopomers is due to “symmetry driven” isotope effects. The asymmetric ozone isotopomers contain a greater density of reactive states as compared to the symmetric. The asymmetric species can distribute energy better and is more likely to couple to the exit channel which leads to a stable molecule. For practical application of the theory it is a requirement that these state densities be known (or calculated) for all isotopomer species of interest, and at high precision. An important quality of the Marcus model is that it provides a theoretical structure for the understanding of quantum state density isotope effects in general, and is not specifically confined to the formation of ozone itself. This feature is important because we are now aware that “mass independent” fractionations occur widely in nature. The theory aids in prediction of where such effects will be likely found, and once found, in rationalizing how they were chemically produced.

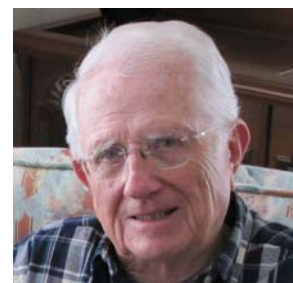
References

1. Alei M, Wagman W (1978) Gas phase ^{13}C chemical shifts and coupling constants in the deuteromethanes. *J Chem Phys* 68:783–784
2. Allison TC, Truhlar DG (1998) Testing the accuracy of practical semiclassical methods: variational transition state theory with optimized multidimensional tunneling. In: Thompson DL (ed) *Modern methods for multidimensional dynamics computations in chemistry*. World Scientific, Singapore, pp 618–712
3. Aston FW (1922) Mass spectra and isotopy. Nobel lecture, December 12, 1922
4. Bardo RD, Wolfsberg M (1965) A theoretical calculation of the equilibrium constant for the isotopic exchange reaction between H_2O and HD. *J Phys Chem* 80:1068–1071
5. Bardo RD, Wolfsberg M (1976) The nuclear mass dependence of the adiabatic correction to the Born-Oppenheimer approximation. *J Chem Phys* 62:4555–4558
6. Bartell LS, Roskos RR (1966) Isotope effects on molar volume and surface tension: simple theoretical model and experimental data for hydrocarbons. *J Chem Phys* 44:457–463
7. Bates FS, Wilthuis P (1989) Spinodal decomposition of a symmetric critical mixture of a deuterated and protonated polymer. *J Chem Phys* 91:3258–3275
8. Bell RP, Coop IE (1938) The dipole moments of hydrogen and deuterium chlorides. *Trans Faraday Soc* 34:1209–1214
9. Benedict M, Pigford M, Levi HW (1981) *Nuclear chemical engineering*, 2nd ed. McGraw-Hill, New York
10. Bigeleisen J (1949) The relative reaction velocities of isotopic molecules. *J Chem Phys* 17:675–679
11. Bigeleisen J (1961) Statistical mechanics of isotope effects on the thermodynamic properties of condensed systems. *J Chem Phys* 34:1485–1493
12. Bigeleisen J (1996) Nuclear size and shape effects in chemical reactions. *Isotope chemistry of the heavy elements*. *J Am Chem Soc* 118:3676–3680
13. Bigeleisen J, Fuks S, Ribnikar SV, Yato Y (1977) Vapor pressures of the isotopic ethylenes. V. Solid and liquid ethylene d1, ethylene d2 (*cis*, *trans* and *gem*), ethylene d3 and ethylene d4. *J Chem Phys* 66:1689–1700
14. Bigeleisen J, Lee MW, Mandel F (1973) Equilibrium isotope effects. *Annu Rev Phys Chem* 407–440

15. Bigeleisen J, Mayer MG (1947) Calculation of equilibrium constants for isotope exchange reactions. *J Chem Phys* 15:261–267
16. Bigeleisen J, Wolfsberg M (1958) Theoretical and experimental aspects of isotope effects in chemical kinetics. *Adv Chem Phys* 1:15–76
17. Born M, Oppenheimer JR (1927) Zur Quantentheorie der Molekeln. *Ann Phys Leipz* 84:457–484
18. Cleland WW (2006) Enzyme mechanisms from isotope effects. In: Cohen A, Limbach HH (eds) *Isotope effects in chemistry and biology*. Taylor and Francis, Boca Raton. Chapter 37, pp 915–930
19. Cleland WW, O'Leary MH, Northrop DB (1977) *Isotope effects on enzyme-catalyzed reactions*. University Park Press, Baltimore
20. Cohen K (1951) *Theory of isotope separation*. McGraw Hill, New York
21. Collins CJ, Bowman NS (eds) (1970) *Isotope effects in chemical reactions*. Van Nostrand Reinhold, New York
22. Cook PF (1991) *Enzyme mechanism from isotope effects*. CRC Press, Boca Raton
23. Cook PF, Cleland WW (2007) *Enzyme kinetics and mechanism*. Garland Science/Taylor and Francis, London
24. Cramer CJ (2004) *Essentials of computational chemistry*. Wiley-VCH, New York
25. Criss RE (1999) *Principles of stable isotope distribution*. Oxford University Press, Oxford
26. DeNiro MJ (1987) Stable isotope and archeology. *Am Scientist* 75:182–191
27. Diehl P, Fluck E, Gunter H, Kosfield R, Seelig J (eds) (1990) *Isotope effects in NMR spectroscopy*. Vol. 22. Springer Verlag, Berlin
28. Dutta-Choudhury MK, Miljević N, Van Hook WA (1982) Isotope effects in aqueous solutions. The hydrophobic interaction. Some thermodynamic properties of benzene-water and toluene/water solutions and their isotope effects. *J Phys Chem* 86:1711–1721
29. Dutta-Choudhury MK, Van Hook WA (1980) Isotope effects in aqueous solutions. 11. Excess volumes in H₂O/D₂O mixtures. The apparent molar volume of NaCl in an H₂O/D₂O mixture. *J Phys Chem* 84:2735–2740
30. Fajans K (1913) Radioactive transformations and the periodic system of the elements. *Ber Dtsch Chem Ges* 46:422–439
31. Fujii Y, Nomura M, Okomoto M, Onitsuka H, Kawakami F, Takeda K (1989) An anomalous isotope effect of uranium-235 in uranium(IV)-uranium(VI) chemical exchange. *Z Naturforsch* 44:395–398
32. Gajewski JJ, Peterson KB, Kagel JR, Huang YCJ (1989) Transition-state structure in the Diels-Alder reaction from secondary deuterium kinetic isotope effects. The reaction of nearly symmetrical dienes and dienophiles is nearly synchronous. *J Am Chem Soc* 111:9078–9081
33. Galimov EM (1985) *The biological fractionation of isotopes*. Academic Press, New York
34. Gao YQ, Marcus RA (2002) On the strange and unconventional isotopic effect in ozone formation. *J Chem Phys* 116:137–153
35. Giauque WF, Johnston HL (1929) An isotope of oxygen, mass 18. Interpretation of the atmospheric absorption bands. *J Am Chem Soc* 51:1436–1441
36. Giauque WF, Johnston HL (1929) An isotope of oxygen, mass 17, in the Earth's atmosphere. *J Am Chem Soc* 51:3528–3534
37. Glasstone S, Laidler K, Eyring H (1941) *The theory of rate processes*. McGraw Hill, New York
38. Gruneisen E (1926) The equation of state for solids. *Hanbuch der Physik* 10:1–59
39. Hansen PE (2006) NMR studies of isotope effects of compounds with intramolecular hydrogen bonds. In: Kohlen A, Limbach HH (eds) (2006) *Isotope effects in chemistry and biology*. Taylor and Francis, Boca Raton. Chapter 9, pp 253–280
40. Harkins WD, Hayes A (1921) The separation of the element chlorine into isotopes (isotopic elements). *J Am Chem Soc* 43:1803–1825
41. Harkins WD, Wilson ED (1915) The changes in mass and weight involved in the formation of complex atoms. (First paper on atomic structure). *J Am Chem Soc* 37:1367–1383
42. Harkins WD, Wilson ED (1915) The structure of complex atoms. The hydrogen-helium system. (Second paper on atomic structure). *J Am Chem Soc* 37:1383–1396
43. Harkins WD, Wilson ED (1915) Recent work on the structure of the atom. (Third paper on atomic structure). *J Am Chem Soc* 37:1396–1421
44. Hengge AC (2006) Secondary isotope effects. In: Kohlen A, Limbach HH (eds) *Isotope effects in chemistry and biology*. Taylor and Francis, Boca Raton. Chapter 39, pp 953–974
45. Hirschi J, Singleton DA (2005) The normal range for secondary Sawin-Schaad exponents without tunneling or kinetic complexity. *J Am Chem Soc* 127:3294–3295
46. Hoefs J (1973) *Stable isotope geochemistry*. Springer Verlag, New York
47. Hoepfner A (1969) Vapor pressure isotope effects. *Angewandte Chem*. English ed. 8, pp 689–699
48. Houk KN, Gonzalez J, Li Y (1995) Pericyclic reaction transition states: passions and punctilios, 1935–1995. *Acc Chem Res* 28:81–90
49. Imre A, Van Hook WA (1996) Liquid-liquid demixing from solutions of polystyrene. 1. A review. 2. Improved correlation with solvent properties. *J Phys Chem Ref Data* 25:637–661
50. Ishida T, Fujii Y (2006) Enrichment of isotopes. In: Kohlen A, Limbach HH (eds) (2006) *Isotope effects in chemistry and biology*. Taylor and Francis, Boca Raton. Chapter 2, pp 41–87
51. Jakli Gy, Juhász P, Jancso G (1983) Deuterium vapor pressure isotope effect in bromoform. *Acta Chim Hung* 114:133–148
52. Jakli Gy, Tzias P, Van Hook WA (1977) Vapor pressure isotope effects in the benzene(B)-cyclohexane (C) system from 5 to 80 degree C. I. The pure liquids B-d0, B-d1, *ortho*, *meta*, and *para* B-d2, B-d6, C-d0 and C-d12. II. Excess free energies and isotope effects on excess free energies in the solutions B-h6/B-d6, C-h12/C-d12, B-h6/C-h12, B-d6/C-h12 and B-h6/C-d12. *J Chem Phys* 68:3177–3190
53. Jameson CJ (2004) Theoretical and physical aspects of nuclear shielding. *Nucl Magn Reson* 33:47–75
54. Jancso G (2003) Isotope effects. In: Vertes A, Nagy S, Klencsar Z (eds) *Handbook of isotope chemistry*. Kluwer Academic Pub, Dordrecht 4:85–116
55. Jancso G, Jakli Gy, Fetzter Cs (1983) Vapor pressure isotope effects of chloroform. *Z Naturforsch* 38A:184–190
56. Jancso G, Rebelo LPN, Van Hook WA (1993) Isotope effects in solution thermodynamics: excess properties in solutions of isotopomers. *Chem Rev* 93:2645–2666
57. Jancso G, Rebelo LPN, Van Hook WA (1994) Nonideality in isotopic mixtures. *Chem Soc Rev* 23:257–264
58. Jancso G, Van Hook WA (1974) Condensed phase isotope effects (especially vapor pressure isotope effects). *Chem Rev* 74:689–750
59. Jancso G, Van Hook WA (1977) ¹³C and ^{33,34}S isotope effects on the vapor pressure of liquid carbon disulfide. *Can J Chem* 55:3371–3376
60. Jancso G, Van Hook WA (1978) The effect of condensation on vibrational anharmonicity as determined by the vapor pressure isotope effect. *J Mol Struct* 48:107–113

61. Jancso G, Van Hook WA (1978-II) Vapor pressure isotope effects in benzene-cyclohexane systems. III. Theoretical analysis. *J Chem Phys* 68:3191–3202
62. King AS, Birge RT (1930) Evidence from band spectra of the existence of a carbon isotope of mass 13. *Astrophys J* 72:19–40
63. Kiss I, Jancso G, Jakli Gy (1976) Goznyomas izotopeffektus es intermolekularis kolcsonhatasok. Akademiai Kiado, Budapest
64. Kohen A (2006) Kinetic isotope effects as probes for hydrogen tunneling in enzyme catalysis. In: Kohen A, Limbach HH (eds) (2006) *Isotope effects in chemistry and biology*. Taylor and Francis, Boca Raton. Chapter 28, pp 743–764
65. Kohen A, Limbach HH (eds) (2006) *Isotope effects in chemistry and biology*. Taylor and Francis, Boca Raton
66. Kooner Z, Van Hook WA (1988) Isotope effects of simple fluids. Pressure-volume-temperature properties of benzene/deuterobenzene, acetone/acetone-d₃, and methanol/methanol-d₁ from 0.1 MPa and 298 K to critical conditions or to 570 K and 6 MPa, whichever is less. *J Phys Chem* 92:6414–6426
67. Lindemann FA (1919) Note on the vapor pressure and affinity of isotopes. *Philos Mag* 38:173–181
68. Lindemann FA, Aston FW (1919) The possibility of separating isotopes. *Philos Mag* 37:523–534
69. Lopes JNC, Padua AAH, Rebelo LPN, Bigeleisen J (2003) Calculation of vapor pressure isotope effects in the rare gases and their mixtures using an integral equation theory. *J Chem Phys* 118:5028–5037
70. Lowe BM, Smith DG (1975) Dissociation constant of benzoic acid in H₂O and D₂O mixtures. *J Chem Soc Faraday Trans* 71:389–397
71. Maciej T, Yamakawa M, Meller J *et al.* (2003) Deuterium isotope effects on hydrophobic interactions: the importance of dispersion interactions in the hydrophobic phase. *J Am Chem Soc* 125:13836–13849
72. Maessen B, Wolfsberg M (1983) Estimation of dielectric shifts in infra-red spectra of pure liquids for use in the evaluation of vapor pressure isotope effects. *Z Naturforsch* 38A:191–195
73. Marcus RA, Coltrin ME (1977) A new tunneling path for reactions such as H + H₂ → H₂ + H. *J Chem Phys* 67:2609–2614
74. Matsuo S, Van Hook WA (1984) Isothermal compressibilities of benzene-h₆, benzene-d₆, cyclohexane-h₁₂, cyclohexane-d₁₂ and their mixtures from 0 to 30 MPa at 288, 298 and 313 K. *J Phys Chem* 88:1032–1040
75. Melander L, Saunders WH Jr (1980) *Reaction rates of isotopic molecules*. John Wiley and Sons, New York
76. Mielke KL, Peterson KA, Schwenke DW *et al.* (2003) H + H₂ thermal reaction: a convergence of theory and experiment. *Phys Rev Lett* 91:063201/1–4
77. Moseley HGJ (1913, 1914) The high frequency spectra of the elements. *Philos Mag* 26:1024–1034; 27:703–713
78. Mulliken RS (1925) The isotope effect in band spectra, parts I, II, and III. *Phys Rev* 25:119–138; 25:259–296; 26:1–34
79. Naude R (1929) An isotope of nitrogen, mass 15. *Phys Rev* 34:1498–1499
80. Northrop DB (2006) Effects of high hydrostatic pressure on isotope effects. In: Kohen A, Limbach HH (eds) (2006) *Isotope effects in chemistry and biology*. Taylor and Francis, Boca Raton. Chapter 32, pp 837–846
81. Paabo M, Bates RC (1970) Deuterium isotope effects and the dissociation of deuterio-phosphoric acid from 5 to 50 deg. *J Phys Chem* 74:706–710
82. Quinn DM (2006) Theory and practice of solvent isotope effects. In: Kohen A, Limbach HH (eds) *Isotope effects in chemistry and biology*. Taylor and Francis, Boca Raton. Chapter 41, pp 995–1018
83. Rabinovich IB (1970) Influence of isotopy on the physico-chemical properties of liquids. Consultants Bureau, New York
84. Raynes WT, Fowler PW, Lazzaretti P, Zanasi R, Grayson M (1988) The effects of rotation and vibration on the carbon-13 shielding, magnetizabilities and geometric parameters of some methane isotopomers. *Mol Phys* 64:143–162
85. Richardson SM, McSween HY Jr (1989) *Geochemistry, pathways and processes*. Prentice Hall, Englewood Cliffs, New York
86. Ridley BA, Schultz WR, Le Roy DJ (1966) The kinetics of the reaction D + H₂ = HD + H. *J Chem Phys* 44:3344–3347
87. Roth JP, Klinman JP (2006) Oxygen-18 isotope effects as a probe of enzymatic activation of molecular oxygen. In: Kohen A, Limbach HH (eds) *Isotope effects in chemistry and biology*. Taylor and Francis, Boca Raton. Chapter 24, pp 645–670
88. Schachtsneider JH, Snyder RG (1963) Vibrational analysis of the n-paraffins. II. Normal coordinate calculations. *Spectrochim Acta* 19:117–168
89. Scharlin P, Battino R (1992) Solubility of 13 nonpolar gases in deuterium oxide at 15 to 45°C and 101.325 kPa. Thermodynamics of transfer from H₂O to D₂O. *J Solution Chem* 21:67–91
90. Scharlin P, Battino R (1994) Solubility of CCl₂F₂, CClF₃, CF₄ and c-C₄F₈ in H₂O and D₂O at 288 to 318 K and 101.325 kPa. Thermodynamics of transfer from H₂O to D₂O. *Fluid Phase Equilib* 94:137–147
91. Shakleton NJ, Imbrie J, Pisais N (1988) The evolution of oceanic oxygen isotope variability in the north Atlantic over the past three million years. *Philos Trans R Soc London, Ser B Biological Sci* 318:679–688
92. Shiner VJ, Rapp MW, Halevi EA, Wolfsberg M (1968) Solvolytic α-deuterium effects for different leaving groups. *J Am Chem Soc* 90:7171–7172
93. Singh RR, Van Hook WA (1987) Excess free energies in solutions of isotopic isomers. III. Solutions of deuterated and protiated polymers. *Macromolecules* 20:1855–1859
94. Soddy F (1913) Inter-atomic charge. *Nature* 92:399–400
95. Stern MJ, Van Hook WA, Wolfsberg M (1963) Isotope effects on internal frequencies in the condensed phase resulting from interactions with the hindered translations and rotations. The vapor pressures of the isotopic ethylenes. *J Chem Phys* 39:3179–3196
96. Stern MJ, Wolfsberg M (1966) On the absence of isotope effects in the absence of force constant changes. *J Chem Phys* 45:2618–2629
97. Streitwieser A Jr, Jagow RH, Suzuki S (1958) Kinetic isotope effects in the acetolyses of deuterated cyclopentyl tosylates. *J Am Chem Soc* 80:2416–2419
98. Swain CG, Stivers EC, Reuwer JF Jr, Schaad LJ (1958) Use of hydrogen isotope effects to identify the attacking nucleophile in the enolization of ketones catalyzed by acetic acid. *J Am Chem Soc* 80:5885–5893
99. Thiemens MH (2006) History and applications of mass independent isotope effects. *Ann Rev Earth Sci* 34:217–262
100. Thiemens MH, Heidenreich JE (1983) The mass independent fractionation of ozone. A novel isotope effect and its possible cosmochemical implications. *Science* 219:1073–1075
101. Truhlar DG (2006) Variational transition state theory and multidimensional tunneling for simple and complex reactions in the gas phase, solids, liquids and enzymes. In: Kohen A, Limbach HH (eds) *Isotope effects in chemistry and biology*. Taylor and Francis, Boca Raton. Chapter 22, pp 577–619

102. Urbanczyk A, Van Hook WA (1996) Continuous dilution differential refractometry at useful precision. Isotope effects on polarizability. A new method to determine excess volumes. Application to (water + deuterium oxide), (acetone + d_6 -acetone) and (water + acetone) at $T = 298.15$ K and $\lambda = (470, 520, 559 \text{ and } 650)$ nm. *J Chem Thermodyn* 28:987–1008
103. Urbanczyk A, Van Hook WA (1996) The correlation of excess molar refraction and excess volume for some binary solutions. A new approach. *J Chem Thermodyn* 28:975–986
104. Urey HC, Brickwedde HG, Murphy GM (1932) A hydrogen isotope of mass 2. *Phys Rev* 39:164–165
105. Urey HC, Lowenstam HA, Epstein S, McKinney CR (1951) Measurement of paleotemperatures and temperatures of the upper cretaceous of England, Denmark, and the southeastern United States. *Bull Geol Soc Am* 62:399–416
106. Urey HC, Teal GK (1935) The hydrogen isotope of mass 2. *Rev Mod Phys* 7:34–94
107. Van den Broek A (1913) Intra-atomic charge. *Nature* 92:372–373
108. Van den Broek A (1913) Intra-atomic charge and the structure of the atom. *Nature* 92:476–478
109. Van Hook WA (1966) Vapor pressures of the deuterated ethanes. *J Chem Phys* 44:234–251
110. Van Hook WA (1970) Kinetic isotope effects: introduction and discussion of the theory. In: Collins CJ, Bowman NS (eds) *Isotope effects in chemical reactions*. Van Nostrand Reinhold, New York. Chapter 1, pp 1–89
111. Van Hook WA (2001) Phase diagrams and thermodynamics of demixing of polystyrene solvent solutions in (T,P,x) space. In: Dadmun MD, Van Hook WA, Noid DW, Melnichenko YB, Sumpter BG (eds) *Computational studies, nanotechnology, and solution thermodynamics of polymer systems*. Kluwer-Academic Press, New York. Chapter 1, pp 1–13
112. Van Hook WA (2004) Isotope separation. In: Vertes A, Nagy S, Klencsar Z (eds) *Handbook of nuclear chemistry*. Kluwer Academic Pub, Dordrecht. Vol. 5, pp 177–212
113. Van Hook WA (2006) Condensed matter isotope effects. In: Kohen A, Limbach HH (eds) *Isotope effects in chemistry and biology*. Taylor and Francis, Boca Raton. Chapter 4, pp 119–152
114. Van Hook WA, Rebelo LPN, Wolfsberg M (2001) An interpretation of the vapor phase second virial coefficient. Correlation of virial coefficient and vapor pressure isotope effects. *J Phys Chem A* 105:9284–9297
115. Van Hook WA, Rebelo LPN, Wolfsberg M (2007) Isotope effects on VLE properties of fluids and corresponding states: critical point shifts on isotopic substitution. *Fluid Phase Equilib* 257:35–52
116. Van Hook WA, Wolfsberg M (1994) Comments on H/D isotope effects on polarizabilities of small molecules. Correlation with virial coefficient, molar volume, and electronic second moment isotope effects. *Z Naturforsch* 49A:563–577
117. Villano SM, Kato S, Bierbaum VM (2006) Deuterium kinetic isotope effects in gas-phase S_N2 and E2 reactions: Comparison of experiment and theory. *J Am Chem Soc* 128:736–737
118. Visak ZP, Rebelo LPN, Szydowski J (2003) The “hidden” phase diagram of water + 3-methylpyridine at large absolute negative pressures. *J Phys Chem B* 107:9837–9846
119. Waldmann L (1943) The theory of isotope separation by exchange reactions. *Naturwissenschaften* 31:205–206
120. Warshel A, Olsson MHM, Villa-Freixa J (2006) Computer simulation of isotope effects in enzyme catalysis. In: Kohen A, Limbach HH (eds) *Isotope effects in chemistry and biology*. Taylor and Francis, Boca Raton. Chapter 23, pp 621–644
121. Wiczorek S, Urbanczyk A, Van Hook WA (1996) Application of interferometric continuous dilution refractometry to some solutions, including isotopomer solutions: isotope effects on polarizability in liquids. *J Chem Thermodyn* 28:1009–1018
122. Wigner E (1932) Crossing of potential thresholds in chemical reactions. *Z Phys Chem B* 19:203–216
123. Wilson EB, Decius JC, Cross PC (1955) *Molecular vibrations. The theory of infrared and Raman vibrational spectra*. McGraw Hill, New York
124. Wolff H, Hoepfner A (1965) Wasserstoffbrückenassoziation und dampfdruck-isotopieeffekt von N-deuteriertem methyl- und athylamin. *Ber Bunsengesell Phys Chem* 69:710–716
125. Wolfsberg M (1969) Correction for the effect of anharmonicity on isotope exchange equilibria. *Adv Chem Ser* 89:185–191
126. Wolfsberg M, Van Hook WA, Paneth P, Rebelo LPN (2010) *Isotope effects in the chemical, geological, and bio sciences*. Springer, Dordrecht
127. Zarzycki R (ed) (2002) *Stable isotopes – some new fields of application*. Polish Academy of Sciences, Łódź



W. Alexander Van Hook was educated at the College of the Holy Cross (BS 1957) and Johns Hopkins University (MS 1960, PhD 1961). After postdoctoral experience at Brookhaven National Laboratory he joined the chemistry department at the University of Tennessee where he is now Ziegler Professor Emeritus. Van Hook's research interests are in isotope effects in condensed phases and polymer solution chemistry.